frontiers in Marine Science

ORIGINAL RESEARCH
published: 30 January 2020
doi: 10.3389/fmars.2019.00744

Enigmatic Deep-Water Mounds on the Orphan Knoll, Labrador Sea

Shawn P. Meredyk[1†], Evan Edinger[1,2], David J. W. Piper[3], Veerle A. I. Huvenne[4], Shannon Hoy[5,6] and Alan Ruffman[7,8]*

[1] Environmental Science Program, Memorial University of Newfoundland, St. John's, NL, Canada, [2] Department of Geography, Department of Biology, and Department of Earth Sciences, Memorial University of Newfoundland, St. John's, NL, Canada, [3] Natural Resources Canada, Geological Survey of Canada – Atlantic, Dartmouth, NS, Canada, [4] National Oceanography Centre, University of Southampton Waterfront Campus, Southampton, United Kingdom, [5] School of Earth Sciences, University of Bristol, Bristol, United Kingdom, [6] Department of Earth Science, University of New Hampshire, Durham, NH, United States, [7] Geomarine Associates, Ltd., Halifax, NS, Canada, [8] Department of Earth Sciences, Dalhousie University, Halifax, NS, Canada

OPEN ACCESS

Edited by:
Vincent Lecours, University of Florida, United States

Reviewed by:
Autun Purser, Alfred Wegener Institute Helmholtz Centre for Polar and Marine Research (AWI), Germany
Andrea Gori, University of Salento, Italy

***Correspondence:**
Evan Edinger
eedinger@mun.ca

†Present address:
Shawn P. Meredyk, Amundsen Science, Quebec City, QC, Canada

Specialty section:
This article was submitted to Deep-Sea Environments and Ecology, a section of the journal Frontiers in Marine Science

Received: *15 June 2019*
Accepted: *14 November 2019*
Published: *30 January 2020*

Citation:
Meredyk SP, Edinger E, Piper DJW, Huvenne VAI, Hoy S and Ruffman A (2020) Enigmatic Deep-Water Mounds on the Orphan Knoll, Labrador Sea. Front. Mar. Sci. 6:744. doi: 10.3389/fmars.2019.00744

Deep-sea mounds can have a variety of origins and may provide hard-substrate features in depths that are normally dominated by mud. Orphan Knoll, a 2 km high bedrock horst off northeast Newfoundland, hosts more than 200 mounds, or mound complexes, of unknown composition, in water depths of 1720–2500 m. Most mounds are 10–600 m high, with average mound height 187 m, and 1–3 km wide. The study objective was to characterize the size, shape, orientation, and composition of the enigmatic Orphan Knoll mounds, in order to determine their age and origin. Archival ship-based side-scan sonar, multibeam sonar, airgun, high-resolution sparker and 3.5 kHz acoustic sub-bottom profiling, and newly acquired ship-based multibeam sonar, video transects by remotely operated vehicle (ROV), rock samples, and near-bottom multibeam sonar data were analyzed. Four mounds were studied during two ROV dives. Archival sidescan sonar data show > 200 mounds. Sparker profiles show that the mound crests are covered by condensed stratified Quaternary sediment and airgun seismic data show faults reaching near the seafloor. New multibeam sonar data show mounds are dominantly conical to elliptical in shape, but without preferred orientation or alignment. Remotely operated vehicle (ROV) transects and near-bottom multibeam showed that three mounds were rounded and symmetrically arranged, while a fourth was more asymmetrical, with steep faces on the southwestern and southeastern flanks, where finely bedded to massive sedimentary bedrock outcropped dipping 15–45°SW. Rock samples from the mounds include Eocene calcareous ooze and mid-Miocene bedded pelagic limestone. Thick ferromanganese crusts were found on many surfaces, obscuring possible outcrops from physical sampling. Polymetallic nodules were found on the slope of one mound. Ice-rafted detritus, including igneous and metamorphic rocks and Paleozoic limestone and dolostone, was common in the sediments immediately surrounding the mounds. Quaternary sub-fossil solitary scleractinian corals accumulated over a span of at least 0.18 Ma at the base of one mound. The presence of uplifted condensed Eocene-Miocene rocks on the mounds and faulting in seismic profiles suggest uplift during

reactivation of old rift-related faults during the Neogene, with seabed mass wasting creating residual mounds, which were then draped by Quaternary proglacial muds. Sculpting of hemipelagic Quaternary sediment by bottom currents probably contributed to mound morphology.

Keywords: Orphan Knoll, deep-sea, mound, multibeam sonar, Northwest Atlantic, cold-water corals

INTRODUCTION

Deep-water mounds are intermediate-scale bathymetric features found in bathyal to abyssal settings, with a wide variety of possible origins. Deep-water mounds are typically 10s to 100s of meters in height above the surrounding sea floor, and may have lateral dimensions of 100s of meters to kilometers, rarely 10s of kilometers. Mounds are larger than sedimentary structures, but smaller than volcanic seamounts, whose definition includes an elevation of 1000 m above the surrounding sea floor, and a conical shape with length/width ratios < 2 (Harris et al., 2014). Deep-water mounds can provide important hard-substrate habitats in environments that are otherwise dominated by soft sediment, hence hosting higher levels of biodiversity, particularly epifaunal and fish biodiversity, than surrounding level-bottom seafloor. In the past 1–2 decades, deep-water mounds built by biogenic processes, especially carbonate mounds, have received greater attention (e.g., Huvenne et al., 2003). Bathyal carbonate mounds were also investigated particularly as a possible modern analog for carbonate mud-mounds in the fossil record (e.g., Henriet et al., 2011, reviewed by Lo Iacono et al., 2018).

The range of biogenic and abiogenic processes responsible for mound formation is considerable. Some examples of the more common abiotic processes of mound formation, include tectonism and block-faulting (e.g., Laughton et al., 1972; Sibuet, 1992; Moscardelli et al., 2013, reviewed by Cormier and Sloan, 2018); magmatic volcanism (e.g., Wiles et al., 2014, reviewed by Casalbore, 2018), and diapirism (e.g., Laughton et al., 1972), often associated with rifting or failed rifts; salt diapirs (e.g., Laughton et al., 1972; Parson et al., 1984), mud volcanoes and similar structures related to fluid escape (e.g., Barrett et al., 1988; Bolton et al., 1988; Enachescu, 2004; Burton-Ferguson et al., 2006, reviewed by Mazzini and Etiope, 2017); cold-seeps and authigenic carbonate precipitation (reviewed by Ceramicola et al., 2018); some types of contourite drifts (reviewed by Esentia et al., 2018) and submerged subaerial erosion features such as karst (Hart, 1977; Parson et al., 1984; Dronov, 1993; Immenhauser and Rameil, 2011; Taviani et al., 2012). Biogenic mounds in the deep sea include, a variety of types of biogenic carbonate mound formation including cold-water coral reefs and mounds (e.g., Hovland et al., 1994; Huvenne et al., 2003; Roberts et al., 2003, 2006, reviewed by Lo Iacono et al., 2018), and siliciclastic-dominated sponge reefs (e.g., Conway et al., 2005; Howell et al., 2016) and microbial mounds (e.g., Riding and Awramik, 2000). The different origins of mounds may or may not yield distinctive morphologies that can be used to interpret the geological origins of the mound features. As is typical for the deep sea, far more mound features have been mapped using acoustic remote sensing than have been directly investigated and sampled.

This paper examines deep-sea mounds of indeterminate origin on Orphan Knoll. The Orphan Knoll mounds were first detected in 1970 (Laughton et al., 1972). Parson et al. (1984) provided a first map and description of the mounds based on side-scan sonar, and analysis of rock dredge samples, and considered various hypotheses for their origin. Interest in Orphan Knoll and the Orphan Knoll mounds re-emerged in the late 1990s and early 2000s when late Pleistocene and Holocene solitary scleractinian corals collected in the 1978 Geological Survey of Canada exploration of Orphan Knoll (Keen, 1978) were re-analyzed for paleoceanographic investigations (e.g., Smith et al., 1997). The cold-water coral research on the Orphan Knoll, combined with previous studies on carbonate rock samples from the Knoll (Legault, 1982; Parson et al., 1984; van Hinte et al., 1995) raised the possibility that the Orphan Knoll mounds were biogenic carbonate mounds (Enachescu, 2004). Accordingly, Orphan Knoll was eventually protected from deep-water fishing activity by a Northwest Atlantic Fisheries Organization (NAFO) closure (Thompson and Campanis, 2007), despite the fact that the nature of the mounds, and the nature of the coral fauna, were not yet well-understood.

In this paper, we report on acoustic mapping and sub-bottom profiling, combined with limited *in situ* investigations, of continental slope-depth seafloor mounds on Orphan Knoll. We combine use of archival and new acoustic mapping of these mounds with the results of ROV dives aimed partly at deciphering the origin of these mounds. We also present preliminary results on the living and sub-fossil cold-water coral species present on the mounds. In addition to describing the mounds and exploring the nature and origin of these features, our results chronicle the evolution of submarine surficial geological survey techniques and geomorphological data collection over half a century. The history of the exploration of these features testifies to the evolution of the disciplines of seafloor mapping and submarine geomorphology.

MATERIALS AND METHODS

Study Area

History of Discovery and Exploration of Orphan Knoll

Prior to the Fall of 1969 Orphan Knoll was not a known feature on the ocean floor off Canada's east coast. It first shows as a single 970 fathom sounding on British Admiralty Chart 2060A in 1917 (British Admiralty, 1917). In the 1960s the International Hydrographic Office (IHO) in Monaco initiated the General Bathymetric Chart of the Oceans (GEBCO). Canada took on the compilation of the bathymetry of the Northwest Atlantic which in the 1960s comprised mainly plotting sheets of raw soundings that

were provided voluntarily by vessels passing through the area. These soundings were initially contoured by an undergraduate student at Dalhousie University, resulting in an oblique view of the whole east coast of North America from 50° N southward to Florida. Canada had not yet charted, or compiled, the bathymetry north of about 49° N and it was necessary to use the raw and unedited data on the GEBCO collected soundings sheet #27 (Deutschen Hydrographischen Institut, 1964). These data yielded severely distorted contours that reflected the NE to SW orientation of the Europe to Canada vessel tracks rather than what might be the true shape of the ocean floor.

A reassessment of the GEBCO lines was undertaken, including the removal of certain vessels' data and the deliberate smoothing of the contours. A large feature emerged as an area of shallower depths some 550 km northeast of the island of Newfoundland. It was in the order of 100 km in size, was rather flat-topped and stood over 1250 m proud at a depth of about 3000 to 1720 m. It was hypothesized that this topographic feature was a continental fragment that had become detached from the European plate as the process of continental drift began to open up the northwest Atlantic and the Labrador Sea. The feature was named Orphan Knoll because it had been left behind, and a brief nomination was sent to the embryonic Deep Sea Drilling Project (DSDP) as a proposed drilling site to prove that it was a continental fragment.

The nomination was successful, in part because 1969 magnetometer data from the French vessel *N/O Jean Charcot V* showed that it was not just a very large igneous plateau, and Orphan Knoll was selected as a DSDP Leg 12 drilling site for the mid-1970 voyage of the *Glomar Challenger* despite there being no pre-drilling site survey available. To aid in site selection, the drilling vessel trailed a 20 cubic inch airgun and ran a continuous sub-bottom and magnetic profile whenever it was underway. On the vessel's initial WNW to ESE traverse across the flat top of Orphan Knoll it quite unexpectedly crossed what appeared to be very narrow 'peaks' of up to 300 m in height at the northeast edge of the Knoll. The selected Site 111 was chosen to be approximately 8 km SW of the 'peaks.' When the Site 111 drill hole was completed the vessel moved to the southwest of the drill hole, streamed the survey gear, and then ran a SW to NE survey line across the Site 111 and on off the Knoll into deep water. Once again the vessel mapped a narrow zone of significant 'peaks' at the northeast edge of Orphan Knoll. The 'peaks' came to be called "narrow ridge-like structures" by the scientific team on board the *Glomar Challenger*. The use of the term 'peaks' was misnomer, in 1970, and today they are now more appropriately called 'mounds.' They were first called 'mounds' by Parson et al. (1984) and then the "Enigmatic Mounds" in Ruffman (2011), as their origin has continued to defy geoscientists.

The final core of DSDP Leg 12, Site 111, took an hour to drill and the bedrock core recovered was only 1 m in length, because the diamond bit was almost worn out. The lowermost recovered bedrock was determined to be a non-marine fluvial sandstone with spores that gave it a Bajocian (middle Jurassic) age. This core confirmed that Orphan Knoll was a foundered continental fragment (Laughton et al., 1972; Ruffman and van Hinte, 1973). The Leg 12 Initial Report contained as its **Figure 2** a newly-compiled bathymetry map covering the whole of the feature from 49°30′ to 52°30′ North and 48°52′ to 48°00′ West. The mid-1971 compilation by Ruffman (Laughton et al., 1972) at a contour interval of 200 m then served science in the area for 29 years prior to the first multibeam bathymetry being gathered over the southeast part of the Knoll in 2000. The 'peaks' found along the northeast side of the Knoll were contoured to indicate that they formed a series of prominent sub-parallel NW-SE "narrow ridge-like structures" – probably bedrock in the (then) view of Ruffman. By the time the Leg 12 report was issued, Ruffman and van Hinte, as members of the Leg 12 shipboard scientific party, were permitted to add an 'Addendum' on p. 80 stating that: "The ridges now appear to be erosional remanants[*sic*] of steeply dipping massive limestone beds" based on their interpretation of the contents of a biologic dredge haul in 1971 from the *USNS Lynch* (Ruffman, 1971; Laughton et al., 1972).

With the completion of the Leg 12 scientific Initial Report (Laughton et al., 1972) Canada's interest in Orphan Knoll seemed to stagnate. However the British Institute of Oceanographic Sciences in 1979 ran a single test line over Orphan Knoll on board the MV *Starella,* and in 1981, on board the MV *Farnella,* ran four more E–W lines (400 km *in toto*) of their Geological LOng Range Inclined Asdic (GLORIA) that produced side-scan sonograms of up to 30 km width. These records were somewhat difficult to interpret but served very well in two papers to demonstrate "that the mounds have a random distribution in an elongate northwesterly trending belt" (Parson et al., 1984, 1985). The British survey found that the mounds ranged in height above the seafloor from 115 to 320 m with their flanks sloping at 15 to 20°. "Almost 250 individual mounds have been identified on top of Orphan Knoll. There is no evidence for a northwest–southeast linear fabric in the disposition of the mounds. Although the overall area of distribution of these features is slightly elongated in a northwest–southeast direction, parallel to the continental margin" (Parson et al., 1984, p. 62).

Parson et al. (1984) dismissed all the suggested origins of the mounds to date and instead suggested: "an interpretation based on an irregular, partially buried palaeolandscape best fits the available evidence." A paragraph later they hedged their bets by adding "Alternatively, the mounds might be erosional remnants of original depositional features of sedimentary rocks" and gave an example, "of reef knolls, [in] the Spanish Sahara. Here, circular reef knolls, preserved due to their greater resistance to erosion than the marls in which they occur, form topographic features up to 2 km in diameter and 100 m in height. Aerial photographs of the reef-knoll terrain. bear a striking resemblance to the GLORIA sonographs of Orphan Knoll" (Parson et al., 1984, p. 66). The Spanish Sahara reef knolls, or *kes-kes*, have been attributed to both shallow- and deep-water corals and carbonate mound formation (Henriet et al., 2014), and were part of the later interest in the Orphan Knoll mounds as possible biogenic carbonate mounds.

A year later Parson et al. (1985) gathered together their thoughts on the regional structural development of the eastern Grand Banks including normal faulting at the ocean-continental transition (OCT). The fault-bounded basin that contains the Middle Jurassic non-marine rocks in a half-graben on top of

Orphan Knoll is interpreted to be probably related to "a tensional episode with graben formation during the Late Triassic and Early Jurassic, rifting and erosion began in the Late Jurassic and continued until the Aptian" (Parson et al., 1985, p. 700). The work of the British in 1979 and 1981 using the towed GLORIA tool to gather seafloor sonograms and sub-bottom profiling data was the last mound-specific survey work done by any research cruise for 23 years.

In 1978 a team from the Bedford Institute of Oceanography (BIO) attempted two rock dredge hauls on one of the mounds located using the 1970 DSDP Leg 12 drill ship echosounder data during the *Hudson* 78-020 expedition. One dredge did not obtain any material that clearly reflected nearby bedrock. The other, however, brought up over 200 pieces of dead, lightly-Mn-coated, *Desmophyllum cristagalli* (now synonimzed to *Desmophyllum dianthus*). The preferred habitat of this azooxanthellate, cold water, solitary to pseudocolonial scleractinian coral is a vertical to slightly over-hanging rock face (Keen, 1978; Ruffman and van Hinte, 1989; Forsterra et al., 2005). No one at BIO was interested in the samples, and the coral remained unstudied and mis-identified for a decade. Eventually the dredge haul was fully examined and Stephen D. Cairns of the Smithsonian Institution in Washington identified the coral recovered as *D. cristagalli*. We concluded that the rock dredge had dragged through a *Desmophyllum* 'graveyard' below a bedrock face hosting living examples of the coral (Ruffman and van Hinte, 1989). This coral collection ultimately was the topic of a B.Sc. Honours and eventually a portion of a Ph.D. thesis at McMaster University, focusing on Quaternary paleoceanographic reconstructions of the Labrador Sea based on the coral skeleton stable isotope geochemistry (Smith, 1993, 1997; Smith et al., 1997, 2013).

The first multibeam sonar data acquired over any part of Orphan Knoll and the Orphan Seamount was obtained almost by accident. The Americans had built the new ice-capable *USCGC Healy,* which was equipped with a 12 kHz Seabeam multi-beam sonar. The vessel was to transit from the Atlantic Ocean to its area of operations in the Beaufort Sea via the Northwest Passage. A testing area for the multibeam sonar was chosen without much thought about the underlying geology of the ocean floor that was to be mapped. The equipment testing cruise covered only the southeastern edge of Orphan Knoll and mainly the abyssal depths of the bordering Labrador Abyssal Plain (Toews and Piper, 2002). Six years later Canada still had no deep-sea vessels in the Atlantic with a multi-beam bathymetry system and in 2006 chartered Fugro's *Kommandor Jack* with its 12 kHz multibeam bathymetry system to run a zig-zag series of check lines along Canada's eastern continental margin, including the Orphan Knoll area (Pe-Piper et al., 2013, 2014). These data were collected to fortify Canada's claim for extended jurisdiction under Article 76 of the United Nations Convention on the Law of the Sea (UNCLOS). Canada finally added a multi-beam sonar system to one of its Arctic-capable icebreakers, *CCGS Amundsen,* in 2003. Despite extensive mapping in the Canadian Arctic and the northern Labrador sea, the vessel has not yet been used to map the bathymetry of Orphan Knoll. To date, the modest amount of *Kommandor Jack* multi-beam data from 2006 comprise the only 'Canadian' swath bathymetry data over any part of Orphan Knoll.

Michael Enachescu (2004) re-examined two commercial Husky Oil deep seismic profiles run in Orphan Basin to the west of Orphan Knoll. These 2000–2003 2D multi-channel seismic lines crossed the western flanks of Orphan Knoll and ran partway onto the flatter top of the feature to the east. Enachescu (2004) identified two features that he called "geo-mounds," which appeared to have possibly grown up through the ca. 150 m of Quaternary hemipelagic sediment cover, and were visible as small "geo-mounds" in the present-day bathymetry. He suggested that these might be bioherms of cold-water corals, and as such Enachescu prompted us all to consider cold water bioherms as the origin of the mounds on the northeast part of Orphan Knoll. In 2004 a brief visit over the top of Orphan Knoll was made by the *CCGS Hudson* 2004-024 cruise. A dredge attempt was made on one of the mounds without any bedrock recovery but a Huntec sparker profile over the mound showed ca. 10 m of stratified sediment draped over the mound crest (as reported in this paper).

In the period 2007–2008 the North Atlantic Fisheries Organization (NAFO) was being challenged to consider the possible need for regulation of fishing effort on any seamounts within its jurisdiction of the Northwest Atlantic (Thompson and Campanis, 2007). The maximum economic depth of possible fishing was considered to be 2000 m. Thus seamounts in the New England Seamount Chain off Nova Scotia and New England, in the Fogo Seamount Group on the southern edge of the Grand Banks and seamounts in the Newfoundland Seamount Group to the east of the southern Grand Banks were all targeted for assessment by NAFO. To NAFO the whole of the top of Orphan Knoll rose above 2000 m – *ergo* Orphan Knoll must be a 'seamount' and it has been mis-named by NAFO ever since. In 2008 NAFO closed the four seamount areas to all fishing (Thompson and Campanis, 2007). This closure and the ensuing Canadian Department of Fisheries and Oceans (DFO) assessment led to a comprehensive measurement and documentation of the physical oceanographic parameters over Orphan Knoll (Greenan et al., 2010), and spurred the biological aspects of the 2010 ROV survey of Orphan Knoll, some of which are reported on in this paper.

There was no further work on the Enigmatic Mounds themselves until the 2010 Bedford Institute of Oceanography and Memorial University *CCGS Hudson*-2010-029 cruise using the tethered *ROPOS* ROV which examined two mounds with video, rock and coral sampling, and a ROV-mounted multi-beam system. Edinger and Sherwood (2012) and Blénet (2016), examine the taphonomy of the corals in this time-averaged assemblage. The 2010 cruise was followed by the 2017 British ICY-LAB Cruise DY081 on *RRS Discovery* which recorded a multibeam sonar survey over the mounds on the northeast portion of Orphan Knoll. The data ROV video observations, rock samples, and near-bottom multibeam bathymetry data from the *Hudson* 2010-029 cruise and the ship-based multibeam data from the 2017 *Discovery* cruise to Orphan Knoll are reported on in this paper.

Geological Background

Orphan Knoll is a flat-topped (∼1700 m) basement high of continental crust separated from the eastern Canadian

continental shelf by the Orphan Basin (2500–3000 m). The Knoll rises 2 km above the adjacent Labrador Sea ocean basin. Orphan Basin was affected by several phases of Mesozoic rifting culminating in the Late Jurassic-Early Cretaceous hyperextension (Enachescu et al., 2005; Dafoe et al., 2017). Continental breakup east of Orphan Knoll followed during the Mid-to Late Cretaceous, with the oldest definite magnetic anomaly on the seaward side of Orphan Knoll being C34n (84 Ma, Santonian, Srivastava et al., 1988). A major fault scarp on the eastern side of Orphan Knoll bounds 40 km of thinned continental crust (Chian et al., 2001; Welford et al., 2012) before oceanic crust is reached. Flemish Cap, 100 km to the south, is an analogous but shallower basement high seaward of the Grand Banks of Newfoundland.

The geological history of Orphan Knoll is known principally from Deep Sea Drilling Project Site 111 drilled in 1970 on the crest of the Knoll (Laughton et al., 1972). Sparsely cored intervals sampled a 150 m thick hemipelagic Quaternary interval (seismic unit 6 in **Figure 4**) overlying very thin Miocene chalk and 30 m of Paleogene zeolitic clays (unit 5) resting on latest Cretaceous chalk (upper part of unit 4). This deeper water succession overlies 50 m of shallow water limestones, of Aptian–Cenomanian (mid Cretaceous) age (lower unit 4), unconformably overlying middle Jurassic (Bajocian) terrestrial sandstones and shales. In seismic profiles these Jurassic strata overlie Appalachian crystalline basement (Enachescu, 2004).

Late Quaternary sedimentation on Orphan Knoll is known from studies of piston cores and from the nearby deeper water Ocean Drilling Program Sites U1302/3 (Channell et al., 2012). Sediments of the last glacial cycle on the crest of the Knoll are about 5 m thick and are predominantly of proglacial origin, including Heinrich layers rich in detrital carbonate rocks derived from Hudson Bay. Ice-rafted detritus is thus rich in Lower Paleozoic rocks and previous accounts of Ordovician and Devonian rocks are probably from icre-rafted boulders.

Mapping

Compilation and Analysis of Archival Mapping Data

Archival acoustic and seismic data sources available for studying the Orphan Knoll mounds included extensive low-resolution GLORIA side-scan sonar data (Parson et al., 1984), Geological Survey of Canada air gun and Huntec sparker seismic data, and isolated swaths of multibeam sonar data covering the Orphan Knoll (**Figure 1** and **Supplementary Material** for individual data layers).

Historical acoustic imagery

Raw survey data (seismic reflection profiles, side-scan sonar and multibeam sonar) from historical cruises were compiled into an ArcGIS project to aid in planning the *Hudson* 2010-029 survey and data interpretation.

Seismic profiles. Hull-mounted Knudsen 3.5 kHz seismic profiles were collected from cruises: 78-020, 86-013, 90-007, 2001-043, 2003-033, 2004-024; 3.5 kHz Knudsen and 3.5 kHz Huntec® sparker profiles were collected from CCGS *Hudson* cruises: 2003-033, 2004-024, and 2010-029; 3.5 kHz airgun seismic profiles were collected from CSS *Hudson* cruise 69-041; LITHOPROBE deep seismic data from line FGP 84-3D, TGS line 107 and GSI lines ORO-111 and ORO-129 were examined and new enigmatic mounds [high slope (>45°)] were recorded and plotted in a ArcGIS project (see **Supplementary Figure 4**).

Side scan imagery. GLORIA (Geological Long Range Inclined Asdic) 6.5 kHz side-scan imagery collected on the *MV Starella* and *MV Farnella* cruises covered ∼40% of the Orphan Knoll, focused on the northern section of the Orphan Knoll (Parson et al., 1984, see **Supplementary Material**). Ridge and mound features were created by geopositioning GLORIA imagery and manually digitizing the mounds and ridges seen in the imagery. See **Supplementary Figures 1**, **2**.

Multibeam bathymetry. In 2000, the United States Coast Guard Cutter (USCGC) *Healy* used a Seabeam 2112 multibeam sonar (12 kHz) and collected bathymetry (gridded to 100 m res.) over the SE-W Orphan Knoll; these data were made available by the Geological Survey of Canada (GSC). See **Supplementary Figure 3**.

In 2006, the Fugro vessel *Kommandor Jack* (*Kmdr. Jack*) was commissioned by Natural Resources Canada to collect data for Canada's claim for extended jurisdiction under the United Nations Convention on the Law of the Sea 's (UNCLOS) Commission on the Limits of the Continental Shelf (CLCS), re-defining areas of the Canadian continental shelf. The *Kmdr. Jack* used a Kongsberg EM 120 12 kHz multibeam unit and collected bathymetry gridded to 100 m resolution over the southeast Orphan Knoll (see **Supplementary Figure 4**). The *Kmdr. Jack* multibeam raster was overlain by *Healy* multibeam raster, due to raster merging inaccuracies [the *Kmdr. Jack* data was less 'clean' (increased interpolation variance) than the *Healy* data] within ArcGIS (inaccuracies were visualized in 3D, using GlobalMapper ver. 11); therefore, rather than merging the rasters, the *Healy* data was overlaid the *Kmdr. Jack* data, to get the most accurate raster for point-sampling statistical purposes.

Acquisition of New Ship-Based Multibeam Bathymetry

In the summer of 2017, approximately 3400 square kilometers of Orphan Knoll were mapped (bathymetry and backscatter intensity) with Kongsberg's EM122 12 kHz multibeam echosounder (MBES) aboard the RRS Discovery (Cruise DY081). These data were collected in support of the first fieldwork component of Isotope CYcling in the LABrador sea (ICY-LAB) project, led by Dr. K. Hendry from the University of Bristol to study nutrient cycling in the North Atlantic. These data were processed during the expedition (using CARIS HIPS and SIPS v8) and gridded to a 25 m × 25 m resolution. The data (both raw multibeam data and gridded products) and further details can be found in the associated Pangaea data release (Hoy et al., 2018).

ROV Dives and *in situ* Observations

Six ROV dives were carried out on Orphan Knoll during the *CCGS Hudson* Cruise 2010-029 in July 2010 (**Figure 1**

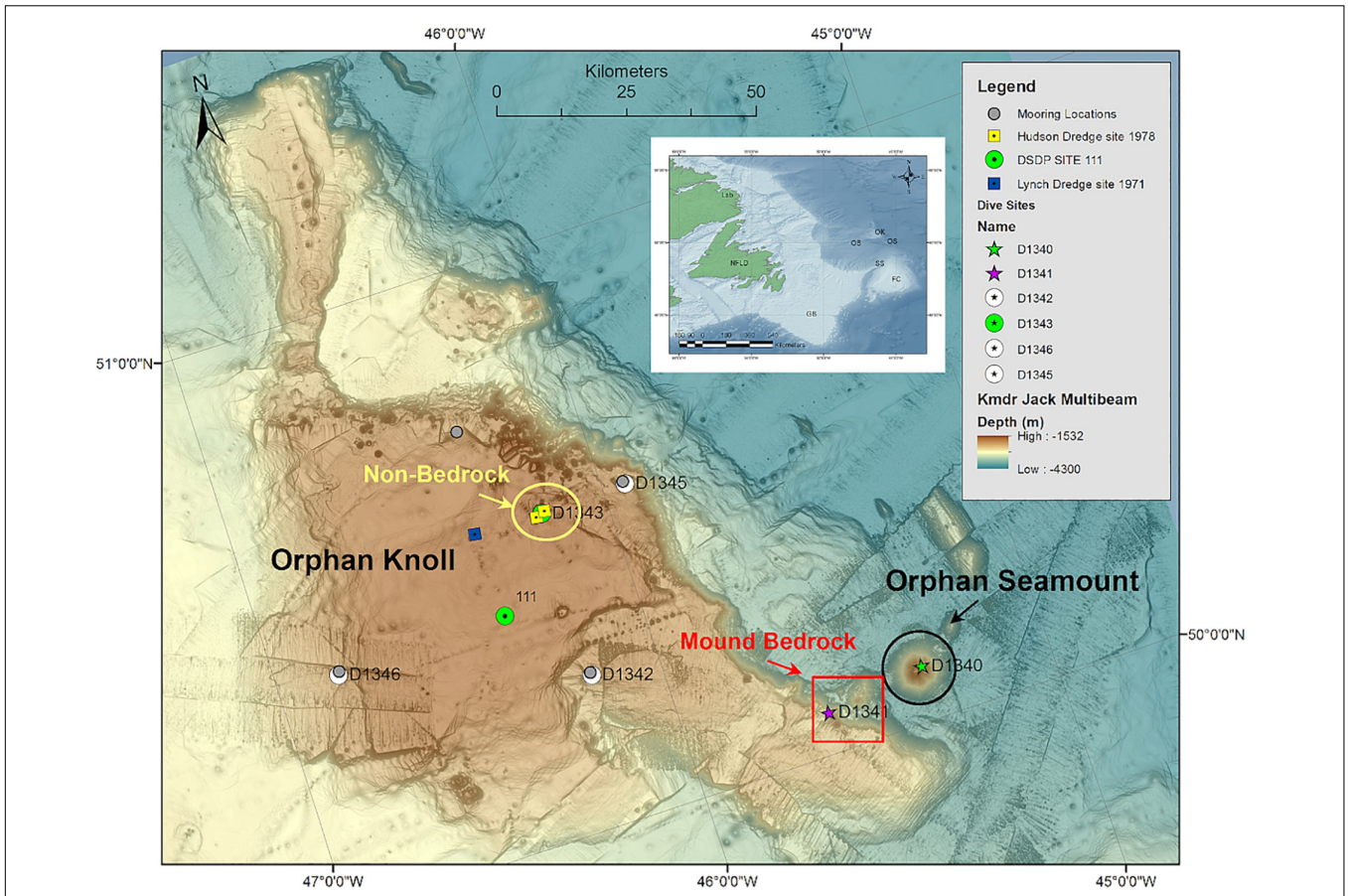

FIGURE 1 | Location of Orphan Knoll and of features studied in detail. Inset map: NFLD, Island of Newfoundland; Lab, Labrador; GB, Grand Banks of Newfoundland; OK, Orphan Knoll; OS, Orphan Seamount; OB, Orphan Basin; FC, Flemish Cap; SS, Sackville Spur. Main figure: Bathymetry is a mosaic of archival multibeam sonar from *USCGC Healy* and *MV Kommandor Jack* data (see **Supplementary Material**) with GEBCO bathymetry for region. Positions of previous drilling (DSDP site 111) and rock dredge sampling (*USNS Lynch*, 1971, *CCGS Hudson*, 1978) also shown, as well as locations or remotely operated vehicle (ROV) dives completed during *CCGS Hudson* 2010-029 mission.

TABLE 1 | ROPOS dives during the *Hudson* 2010-029 mission.

Dive #	Date	Start lat	Start long	Max depth (m)	Min depth (m)	Duration (h:m)	Distance surveyed (km)	Principal objectives
R1341	20 July 2010	N50° 04.5695′	W45° 37.301′	2895	2344	15:25	3.8	Survey SE Orphan Knoll mounds
R1342	21 July 2010	N50° 15.8704′	W46° 11.1371′	2195	2150	9:00	Not linear survey	Search for lost current meter mooring, collect sediment cores
R1343	22 July 2010	N50° 33.8078′	W46° 10.3591′	1852	1682	15:51	5.35	Survey NE Orphan Knoll mounds, collect fossil corals
R1344	23 July 2010	N50° 34.1167′	W45° 54.164′	n/a	n/a	3:35	0	Bottom type and biological survey of NE Orphan Knoll curremt meter location.
R1345	23 July 2010	N50° 33.4792′	W45° 55.6297′	2370	2240	7:34	3.5	Bottom type and biological survey of NE Orphan Knoll curremt meter location
R1346	24 July 2010	N50° 23.8483′	W46° 50.7028′	2270	2162	9:34	4.65	Bottom type and biological survey of SW Orphan Knoll curremt meter location

Remotely operated vehicle dives on the Orphan Knoll during the 2010 CCGS Hudson cruise. Depth minima and maxima refer to bottom depths, as opposed to water column observerations, Dive R1344 aborted due to ROV technical issues. Only dives R1341 and R1343 are important for understanding the geology of the Orphan Knoll mounds.

and **Table 1**). Dives R1341 and R1343 were planned in order to investigate and sample mound features on Orphan Knoll. Dives R1342, R1344, 1345, and 1346 were planned to describe bottom type and benthic fauna in the vicinity of four current meters that had been deployed on Orphan Knoll by Fisheries & Oceans Canada in 2009 (Greenan et al., 2010). Three of

these current meters were recovered during the cruise; the current meter at site R1342 was not located. The start and end positions, bottom depth ranges, and durations of the six ROV dives are indicated in **Table 1**. Results relating to the Orphan Knoll mounds relate mostly to dives R1341 and R1343. Dive R1344 was aborted due to ROV malfunction, and yielded no scientific results.

During the *CCGS Hudson* 2010-029 expedition, ROPOS was equipped with two high-definition (HD) (forward facing 1080p HD camera and a downward facing 1080i HD camera) and one 5 Megapixel (MP) digital still camera. Both HD cameras had zooming capabilities with green laser sights 10 cm apart to provide scale at variable zoom distances. The forward facing camera had pan and tilt capabilities while the downward facing camera was affixed to the frame with only tilt functionality, but provided a quantitative view of bottom composition and benthos. Unfortunately, after dive R1340 on the Orphan Seamount (see Pe-Piper et al., 2013), moisture was observed inside the forward-looking HD camera. Therefore the forward-looking HD camera was replaced with the old 3-CCD camera aboard ROPOS, recording data in standard definition, for the remainder of the cruise. The high-definition downward-looking camera remained in operation for the duration of the cruise.

Rock Sample Collection

Ice-rafted debris (IRD) has accumulated on the OK since the initiation of glaciations in the North Atlantic Ocean [Piacenzian (∼3 Ma)] (Hiscott et al., 1989); therefore, positive discrimination of bedrock from ice-rafted boulders could only be verified through *in situ* video, photographs and substrate samples.

Bedrock samples were collected by ROPOS when bedrock outcrops were physically accessible to the ROV and when there was enough room for rock storage within the collection boxes on ROPOS. A CH-15 Stanley underwater chipping hammer clamped to spring-loaded metal rods was installed onto ROPOS for the purpose of chipping sections of bedrock without over-stressing the manipulating arms of ROPOS and to allow ROPOS to collect the sample with its restricted manipulator arm gape (cobble sized rock samples) (**Figure 2A**).

Unfortunately, the shaking of the manipulator arm caused by the chipping hammer limited its use, out of concern for the safety of the manipulator arms and the ability to proceed with other ROV dive objectives. Therefore most of the rock samples were collected by using the ROV manipulator arms to break pieces of bedrock outcrop (**Figure 2B**). Rock samples collected were analyzed by thin-section analysis and x-ray diffraction to study mineralogy, as appropriate.

Bedrock Composition and Structural Observations

The position of ROPOS was plotted within GlobalMapper ver. 11 software by inputting the position data (decoded audio signal from the HD video) from a Geostamp® decoder. Strike measurements were made by observing the heading, pitch and roll of ROPOS, allowing the observer to identify the bedding strike. Dip measurements were made by observing a feature in multiple directions (forward and downward camera perspectives) while being mindful of ROPOS's heading, pitch and roll.

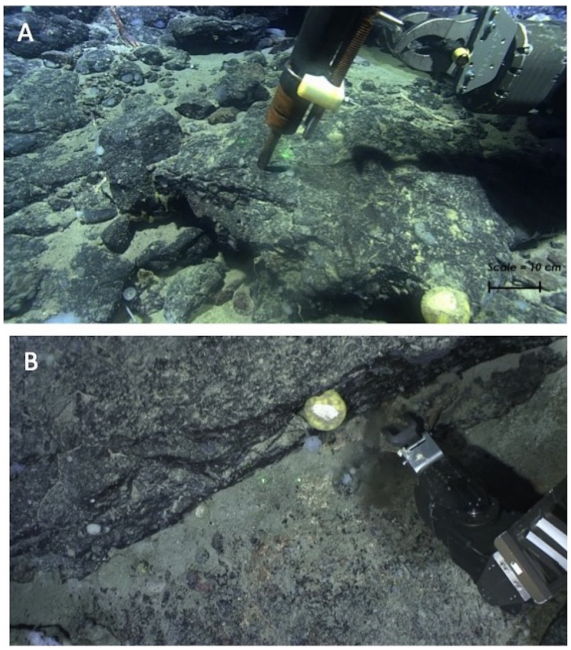

FIGURE 2 | Bedrock sampling from the ROPOS ROV. **(A)** Stanley CH15 hydraulic chipping hammer installed on ROPOS, sampling basalt bedrock on Orphan Seamount (ROPOS dive R1340, Pe-Piper et al., 2013). **(B)** Collecting a rock sample with the ROV manipulator arm, ROPOS dive R1341, SE Orphan Knoll. Note that because the rock samples were picked, rather than broken directly from exposed bedrock, there was greater risk of either collecting ice-rafted debris mistaken for bedrock, or of collecting Fe–Mn oxide crusts from the surface of bedrock exposures.

ROV-Based Near-Bottom Multibeam Sonar Acquisition and Processing

An Imagenex model 837A "Delta T" multibeam unit using 120 beams (3°) at 260 kHz with 0.2% spatial range resolution (res.) (e.g., 2 mm res. at 1 m altitude to 30 mm res. at 15 m altitude) was forward mounted on the ROPOS ROV and calibrated by the Canadian Hydrographic Service (CHS) and the ROPOS engineering team. In addition to measuring small-scale bathymetry along the path of video transects (reported in Lecours et al., 2019), high-resolution maps of two mound features were recorded using the Imagenex Delta T with the ROV at 20 m off bottom. These features were recorded on the second mound observed on dive R1341, and on the principal mound targeted by dive R1343 (see **Table 1**). The Imagenex multibeam data was preliminarily processed on-board and then extensively post-processed (beam and angle elimination were used to 'clean-up' the data; ∼5% beam rejection) using CARIS HIPS & SIPS version 7 (service pack 3). The multibeam unit recorded backscatter data as well; however, due to the ROV flying close to the ground with a high output signal, there was too much acoustic energy ('washed out') to create a color gradient. CARIS image exports were created using 25 cm spatial resolution to smooth fine-scale artificial features within the data, to have the most accurate

bathymetry capable. The raster exports, of the exposed enigmatic OK mounds, were exported from CARIS (ASCII format) and converted by ArcGIS 3D Analyst extension, into an ArcGIS raster grid at 25 cm grid size. In order to visually highlight the small-scale topographic features on these mounds, the bathymetric raster was converted to a slope raster, and the bathymetric raster was draped over the slope raster.

Biological Observations of Cold-Water Corals

The primary goal of biological observations of cold-water corals in this study was to investigate the role of bedrock and surficial geology in influencing benthic faunal distributions. Biological analysis of Orphan Knoll fauna was focused on sessile and sedentary benthic invertebrates, especially cold-water corals and sponges, due to their importance as Vulnerable Marine Ecosystem indicator taxa. Corals and sponges were identified visually where possible, using regional coral identification guides (Kenchington et al., 2009; Wareham, 2009), to the highest taxonomic level possible. The video acquisition and annotation team at sea always included two scientists familiar with coral identification on each watch. In cases where the scientists at sea were uncertain about the identity of a coral, a sample was collected for skeletal or sclerite analysis.

Taxa were identified mostly from the forward-looking camera, and were quantified using the downward-looking camera.

ROV Video Post-processing and Analysis

The HD video was geo-referenced using a Geostamp® device, which audio-encoded the geographic position into the HD video signal\stream. The time-stamped geo-referenced HD video allowed for accurate (1 m spatial resolution) positioning of species relative to surficial geology percentages *in situ* and during re-processing of the HD video. The video annotation program ClassActMapper (CAM) was used during the cruise and in the post-processing of the HD video data to collect geospatial positioning of species relative to surficial geology percentages *in situ* and during re-processing of the HD video. CAM is a graphical user-interface (GUI), whereby the user pressed custom-made species labeled buttons for each instance that a species was seen within the video. The resulting MS Access database contained when and where a species was observed relative to the surficial geology percentages *in situ* and during re-processing of the HD video.

The collective (totaling 100% coverage) surficial geology was recorded every second by CAM using visual estimates and a slider bar of the following sediment size classes, based on the Wentworth scale: bedrock, boulders, cobbles, pebbles, granules, and fine-grained sediment (Sand-Mud). Sand and mud were undistinguishable by eye and were therefore grouped as fine-grained sediment.

The annotations were stored in a MS Access® 97-2003 database and are linked through a post-processing field (JDayGMT) that combines Julian Day and Universal Coordinated Time (UCT). A secondary post-processing of the HD video was performed by a single user to eliminate multi-person estimation variation. The user performed a self-calibration (10 random frame grabs were analyzed using area sampling within ImageJ and compared to the user's estimates to ensure accuracy and precision of their estimates) to determine the offset between the computer calculated percentage and the user's estimate.

Coral Distribution in Relation to Bedrock and Surficial Geology

The location that each coral was observed was noted in the dive log, and was linked via timestamp to the bedrock and surficial geology observations in Class-Act Mapper. The distributions of corals in relation to mounds and bottom type are presented in map form. Quantitative analysis of the relationship between benthic fauna and surficial geology will be published separately.

Geomorphological Analysis of 2017 Bathymetry Data

The 2017 MBES survey carried out during the ICY-LAB expedition covered ca. 3430 km^2 of the Orphan Knoll and Orphan Seamount complex, and mapped out a large number of the enigmatic mounds in great detail. In order to summarize their morphological characteristics, mounds were extracted automatically from the bathymetry (**Supplementary Figure 5**). All data operations and analysis were carried out in ArcGIS v10.5. We used a top-hat transformation (as discussed by Huvenne et al., 2003) with a circular kernel of 40 pixels to single out the mounds. Following the closing operation, mounds were separated from their background at a threshold of 35 m. An additional erosion (3 × 3 pixels) and dilation (5 × 5 pixels) operation was applied to remove fine-scale noise. The resulting binary mask was used to extract the basic metrics of the mounds. Only mound features associated with the main plateau of the Orphan Knoll were retained for further analysis. Mound length and width were defined as the two horizontal dimensions of their bounding rectangles.

Mound orientation was measured according to the azimuth of the longer of the two bounding rectanges, and a histogram of mound orientations constructed on a 180°N–S half-rose diagram. No automated detection of mound alignment was attempted. Instead, possible (speculative) mound alignments were identified visually, as cases where a minimum of four mounds were observed to be aligned following approximately linear trends.

RESULTS

Compilation and Analysis of Archival Acoustic Data

The compiled and mosaicked archival multibeam sonar data from the *USCG Healy* and *Kommandor Jack*, mosaicked with GEBCO bathymetry, revealed the general bathymetry of the Orphan Knoll, and the location of some of the mounds, but provided limited details about the morphology of most mounds, due to the 100 m pixel size in both multibeam data sources (**Figure 1**). Furthermore, the multibeam data were collected in

isolated swaths (see **Supplementary Material**), with more detail on the Northeast edge of the Knoll, and more interpolated data in the center of the Knoll, smoothing the small- to intermediate-scale bathymetric variation necessary for describing the morphology and morphometry of the mounds.

Compilation and Mapping of Mounds in Multibeam Sonar, Side-Scan Sonar, and Sub-Bottom Profile Data for Mound Detection

The compiled data sources detected over 200 mounds (**Figure 3**). The resolution of the archival data, particularly the archival GLORIA side-scan sonar data, allowed for identification of the mounds, and to a much lesser extent, shape. The archival sub-bottom profile data generally allowed for detection of positive relief features that included mounds, but likely also included other unrelated relief features. Most importantly, the sub-bottom profile data allowed for interpretation of mound structure, but not for shape analysis.

Analysis of Mounds in Sub-Bottom Profile for Mound Structure

A few of the mounds on northeast Orphan Knoll are crossed by airgun and sparker single-channel seismic profiles (**Figure 4**). Mounds have steep sides that are masked by hyperbolic diffractions and seismic profiles are cluttered by side-echos from mounds. One mound crossed directly by the ship shows at least 10 m of stratified parallel reflections over its flat crest (**Figure 4A**). In the airgun seismic profiles (**Figure 4C**), interpretation of seismic stratigraphy is difficult, but the most westerly mound imaged appears to have a condensed Quaternary and Cenozoic section over basement, based on seismic character compared to the vicinity of DSDP Site 111. Between the mounds, particularly on the E–W track segment, subvertical faults cut the stratified Cenozoic and Quaternary section between the mounds, and the mounds themselves appear to be fault bounded (**Figure 4C**).

New Multibeam Sonar of Northeast Orphan Knoll Mounds From DY081

The automated mapping exercise based on the ICY-LAB bathymetry data revealed 198 positive bathymetric features (**Figures 5A,B**). Their main morphological characteristics are presented in **Figure 5C**, and summarized in **Table 2**. There was no preferred orientation of mounds, nor was any large-scale alignment of mounds apparent, except where mounds have apparently coalesced near the northern edge of Orphan Knoll (**Figure 5B**). At a smaller spatial scale, visual interpretation suggested that mounds may be aligned following dominantly N–S trends in the southern end of the area mapped (**Figure 5D**).

Overall, mounds are conical to only slightly elliptic (length/width ratios ∼1.5), with an elongation either in roughly N–S or E–W direction (**Figure 5C**). The morphological distributions are strongly skewed, with a lot of small mounds and fewer large features. Based on length and height values, the OK mounds are typically quite steep.

Detailed bathymetry and bathymetric profiles of several mounds close to the zones of ROV exploration are shown in **Figures 6**, **7**. The mounds profiled are clustered, and are broadly conical in shape (**Figures 6A**, **7A**), and had slightly concave to slightly convex curvature (**Figures 6B**, **7B**).

Near-Bottom Multibeam Sonar Records of Mounds and Ridges

Near-bottom (20 m altitude) mapping of a mound on the southeast tongue of Orphan Knoll found the summit of one knoll to be roughly conical to dome-shaped on dive R1341 (**Figure 6**). Mounds on northeast Orphan Knoll were domal to conical in 25 m grid bathymetry, but detailed near-bottom bathymetry revealed more complex features (**Figure 7**).

Southeast tongue of Orphan Knoll, R1341

Near-bottom (20 m altitude) mapping of the mound at the end of dive R1341 showed the summit of this mound to be symmetrical and domal in shape, despite uncorrectable artifacts in the data, probably related to the relatively low frequency of ROV navigation data (0.2 Hz) compared to the MBES acquisition (**Figure 6**). The approximately dome-shaped bedrock outcrop on this mound did not provide clear exposures of stratification within the bedrock of which this mound is composed. The near-bottom bathymetric profile across the mound was measured parallel to ROV motion in order to avoid influence of artifacts on the profile data.

Northeast Orphan Knoll mounds, R1343

The zone investigated by dive R1343 had several large mounds (**Figure 7A**), of which two were surveyed. Detailed near-bottom mapping of the southern end of a large mound surveyed at the end of dive R1343 focused on the area of the coral graveyard collection. The flank of the mound portion mapped at low altitude was generally ridge-shaped (**Figure 7C**). The portion of the mound mapped included extensive stratified bedrock exposure on both the SW and SE flanks of the mound ridge (**Figures 8A–C**). The strike and dip of these bedrock exposures are indicated (see section "Bedrock Structure and Orientation," below). The southern portion of this mound was found to be asymmetrical, with a steeper, concave, face to the southwest, and gentler, linear or convex, bathymetric profiles to the southeast and north (**Figures 7C,D**). Depressions and erosionally accentuated limestone beds were observed within the ROPOS HD video, on and around the OK NE mound, and were also recorded within the ROPOS collected multibeam imagery (**Figures 8A–C**). The concave faces of the mound flank may be attributable to small slope failures, of which three are suggested in the near-bottom multibeam bathymetry, two on the SW side of the mound and one on the southeast side (**Figure 7C**). An approximately north-south oriented linear trough was observed near the crest of this ridge.

ROV Dives and *in situ* Observations

Bedrock Structure and Orientation

Mound bedrock was observed in several locations during dive R1341, most notably in segments A–A, B–C, C′–D′, and G′–H (**Figure 9A**). Despite the extent of these bedrock exposures, none of these outcrops revealed three-dimensional exposures that allowed for examination of bedrock structure.

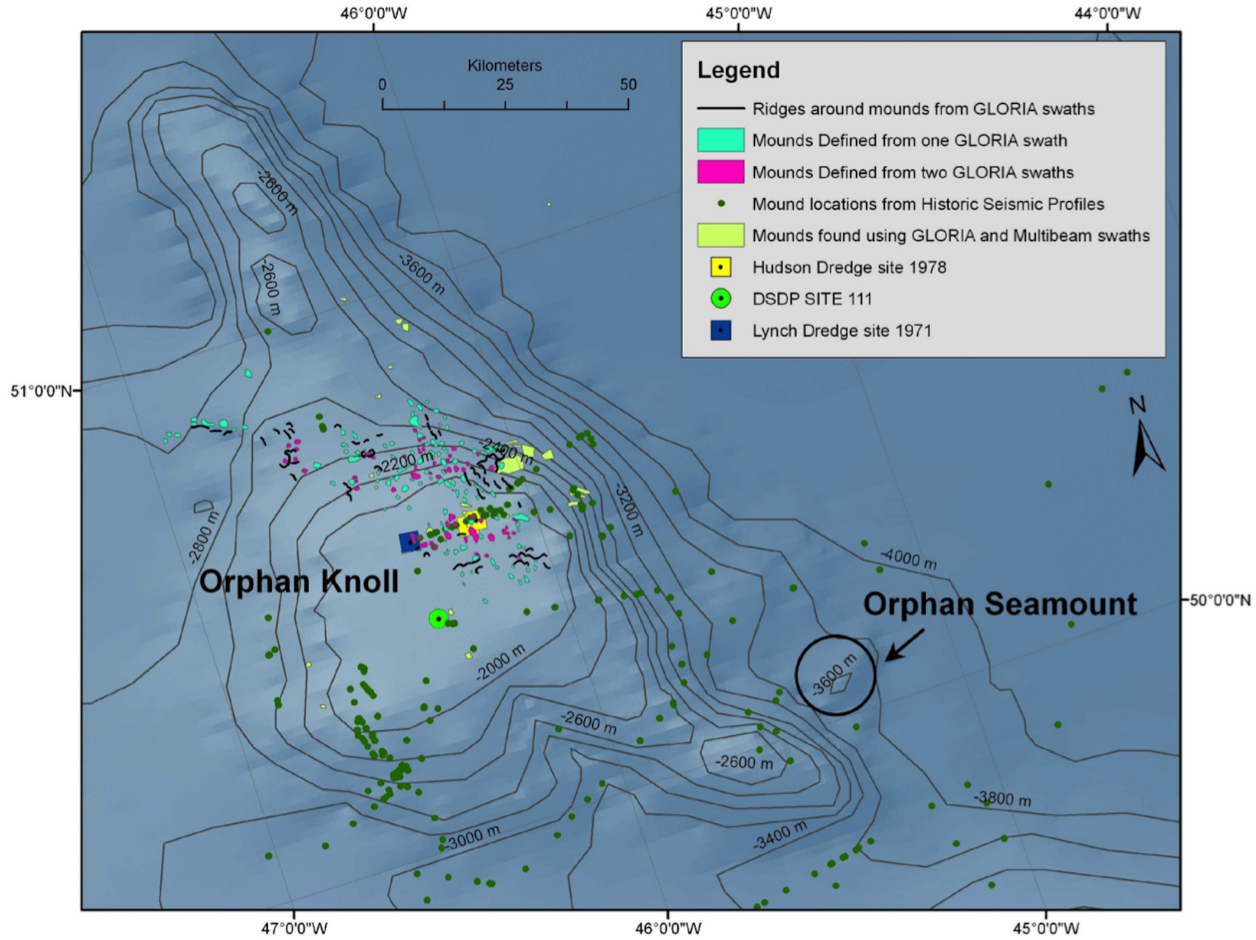

FIGURE 3 | Compilation of mound occurrences from GLORIA side-scan sonar, *USCG Healy* and *Kommandor Jack* multibeam sonar. Green dots represent positive relief features from various legacy Geological Survey of Canada sub-bottom profile data. The apparent alignment of positive relief features from historical seismic profiles is an artifact of linear data acquisition. Orientation and distribution of the various datasets contributing to this figure are presented in **Supplementary Material**.

The bedrock in segments A–A′ consisted of soft carbonate ooze, and polymetallic nodules were observed and collected at the base of this outcrop. The ooze at this outcrop was soft and easily collected with the ROV manipulator arms, in contrast to all other bedrock exposures, which were well-indurated bedrock.

The most extensive ROV observations of Orphan Knoll mound bedrock structure and composition were made during ROV dive R1343 on the northeast Orphan Knoll mounds. **Figure 9B** shows the distribution of bedrock exposures along the track of dive R1343. Along the track of dive R1343, zones with extensive bedrock exposure were found in segments A′–B and E–E′ of the dive. The clearest exposure of stratigraphy within bedrock was found around the SE and SW sides of the mound in segment E–E′ of the dive, near the site from which subfossil corals were dredged in 1978, and collected again in 2010.

Two extensive (250 m long) bedrock outcrops, approximately 250 and 500 m long (**Figure 9B**, surficial geology unit (SGU) A′–B and E–E′) were observed on dive R1343. These were thought to be two mound structures seen in legacy seismic-reflection and side scan imagery (see **Figure 4** and **Supplementary Figures 1**, **2**). Video analysis from SGU E-E' identified exposed bedrock walls on the NW and SE sides of the exposed bedrock outcrop (**Figures 7C**, **10**). The wall feature on the NW side was overlain by fine-grained sediment, while the SE side of the mound consisted primarily of bedrock and granules. The stepped nature of the sedimentary bedrock walls indicated differential erosion, most likely by near-bottom currents.

The most detailed description of stratigraphy and bedrock structure within a mound was possible in segment E–E′ of the mound in dive R1343 (**Figures 7C**, **10**). An unconformity was seen in the larger bedrock outcrop (NE OK mound) between units 2 and 3 (**Figure 10**). The upper bedrock layers (layers 1 and 2) dipped 25–45° with a strike of 135° (SW-NE) (**Figures 7C**, **10**). Unit 1 had thinner bedding than unit 2, while unit 2 had thinner bedding than unit 3. Unit 3 had a different strike and dip than units 1 and 2, probably indicating an unconformity; however, the horizon of the unconformity was covered by overlying IRD, talus and fine grained sediment (**Figure 9**).

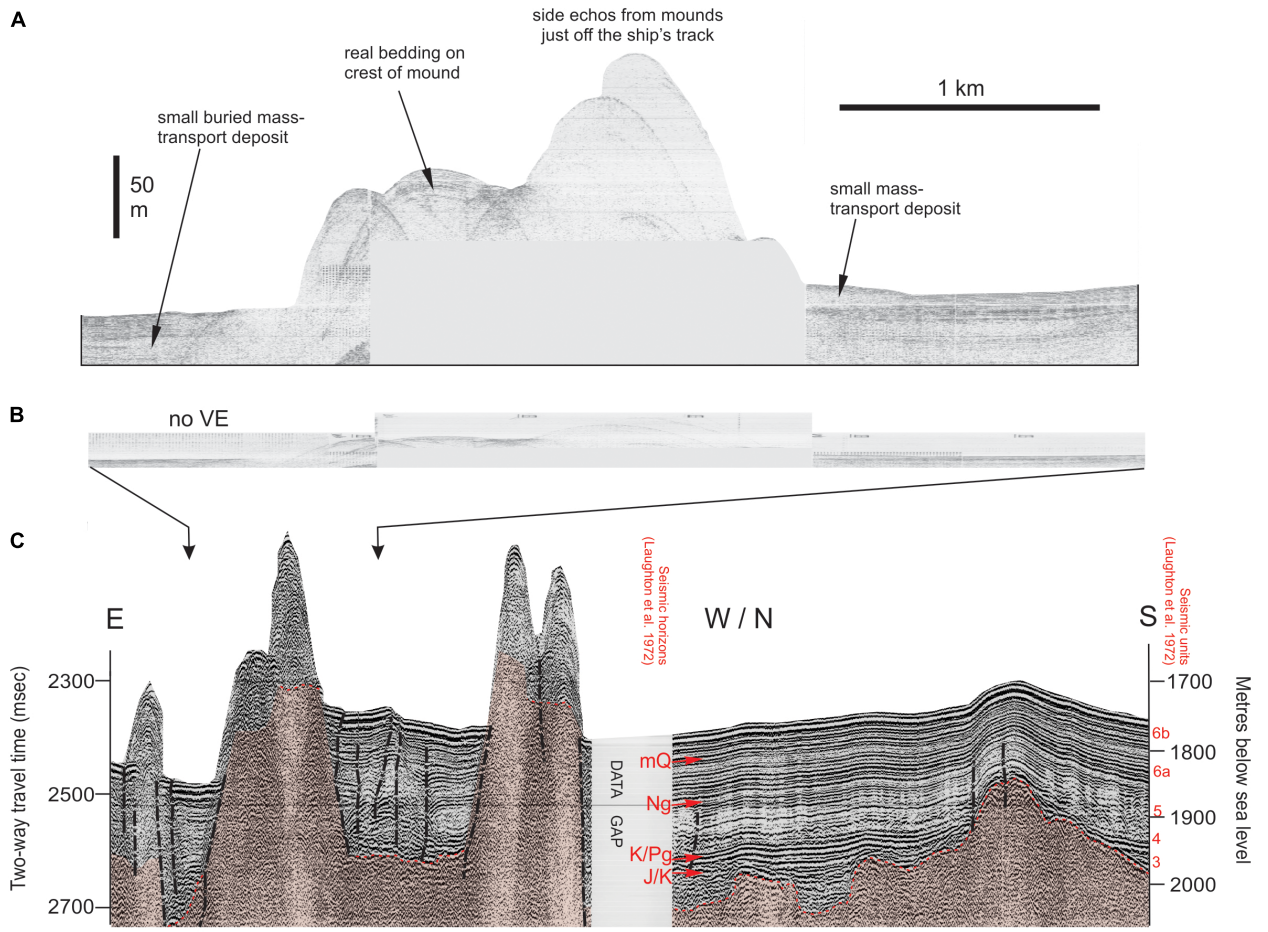

FIGURE 4 | Seismic profiles across mounds on northeast Orphan Knoll (**A**, top panel). Huntec sparker profile across a cluster of mounds showing > 10 m stratified sediment on one mound crest and small mass-transport deposits on the mound flanks **(B,** middle panel). The above profile shown with no vertical exaggeration (**C**, lower panel). 40 cu in GI gun seismic profile showing several mounds, with faulting in stratified section between the mounds. S end of the profile is 5 km north of DSDP Site 111. 3, 4, 5, 6a, 6b are seismic units from Laughton et al. (1972). mQ, mid Quaternary marker (?ca. 1Ma); Ng, thin Neogene (Miocene) unit; K/Pg, Cretaceous-Paleogene boundary; J/K, Jurassic-Cretaceous unconformity. All images from CCGS *Hudson* cruise 2004-024. See **Figure 5B** and **Supplementary Figure 4** for location of seismic profiles shown.

Mound bedrock dips varied between 0 and 45°, accompanied by a general strike of 325° (SW-NE) (**Figure 7C**). However, three strike and dip measurements at the NE OK mound indicated a general strike of 225 and a 0–20° dip. This change in strike and dip possibly indicates an undetected unconformity above unit 3 (**Figure 12**).

Rock Sampling

Due to the intense vibrations induced in the ROV manipulator arm by the hydraulic jackhammer, efforts to sample the bedrock composing the Orphan Knoll mounds were largely unsuccessful. Although we attempted to break off pieces of bedrock with the ROV manipulator arms, most samples collected from bedrock outcrops were thick Fe–Mn crusts, often interbedded with pelagic limestones (see **Supplementary Table 1**). Ice-rafted debris of all size classes was common on all ROV dives. The exceptions to this pattern were the collection of weakly lithified calcareous ooze at the deeper of the two mounds sampled on dive R1341, and collection of pelagic limestones on the shallower of the two mounds studied on dive R1341. Other rock samples included ice-rafted debris collected with sub-fossil deep-sea corals from the sides of the mound studied in dive R1343.

Calcareous ooze with polymetallic nodules

At the beginning of dive 1341, weakly indurated calcareous ooze (R1341-4) and round Fe–Mn nodules (samples R1341-3 and -5) were recovered at the base of an ∼7 m high calcareous ooze outcrop (**Figure 8D**) on a 6° slope near the base of one of two mounds studied on dive R1341. The calcareous ooze sample R1341-4, contained nannofossils *Discoaster sublodoensis, Nannotetrina fulgens*, *Discoaster kuepperi,* and *Discoaster lodoensi* (**Figure 8F**). Nannofossil recovery was good but preservation was poor with extensive etching (central structure of most coccoliths were missing). Some hydrodynamic sorting was evident as only medium to large sized nannofossils were found, though smaller fossils could be absent due to dissolution. No definite recent

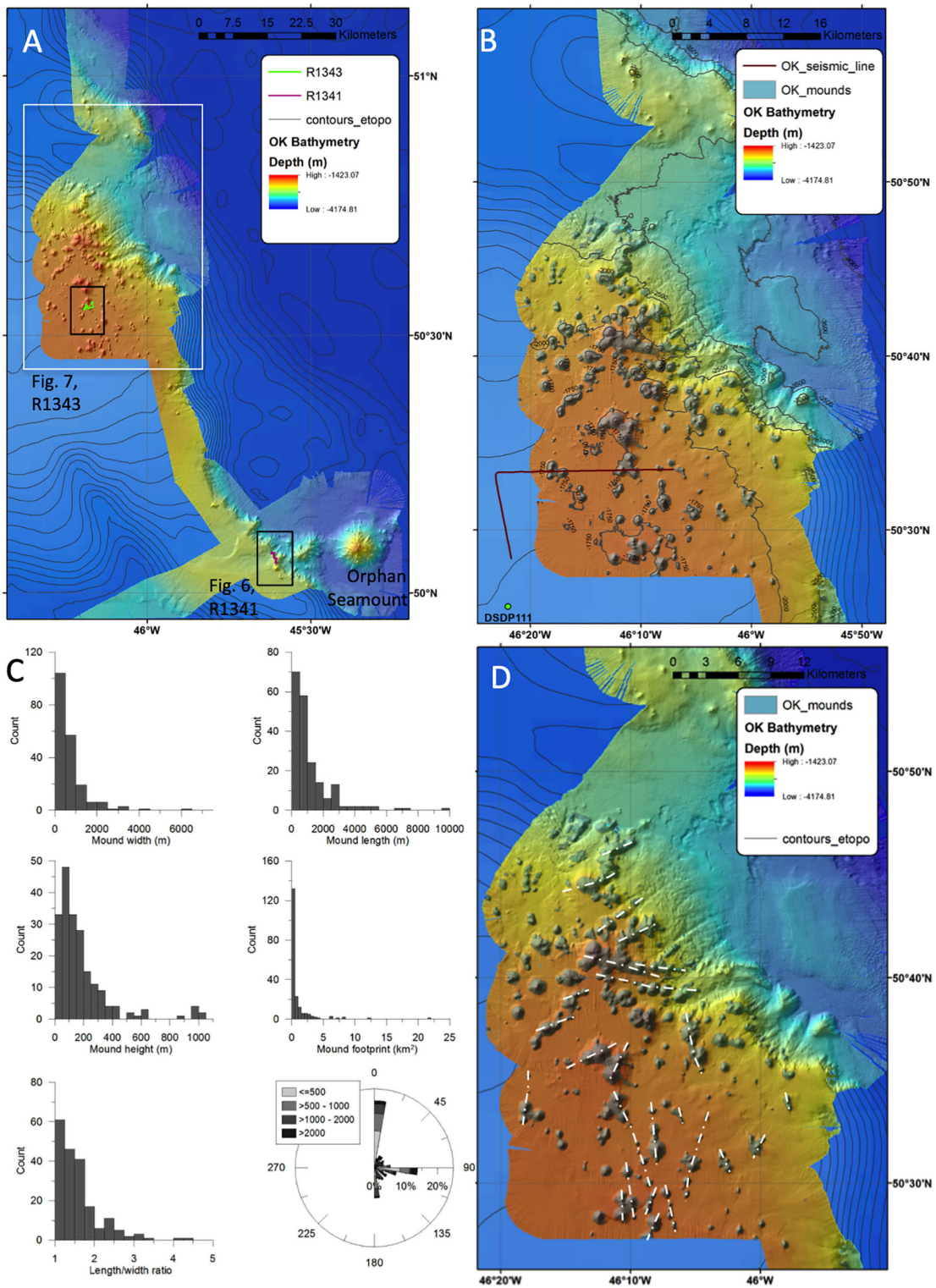

FIGURE 5 | (A) Overview map of the ICY-LAB bathymetry data set over Orphan Knoll. White box indicates are enclosed in right-hand panel **(B)**. Two dark boxes indicate close-up bathymetry shown in **Figures 6A**, 7A. **(B)** Zoom on the central part of the map, illustrating the results of the automated mound mapping exercise over northeast Orphan Knoll. Also shown are the locations of the sub-bottom profile line in **Figure 4**, and the location of DSDP site 111. **(C)** Mound characteristics: histograms of mound width, length, height, footprint area, and length/width ratio. The rose diagram illustrates the orientation of mound elongation, grayscale-coded by mound length in m. **(D)** Speculative linear trends exhibited by groups of mounds. Trends in the southern part of the data set are parallel to the orientation of faults interpreted from seismic reflection profiles.

TABLE 2 | Main morphological characteristics of the 198 Orphan Knoll mounds, measured from the DY081 multibeam sonar survey.

	Width (m)	Length (m)	L/W ratio	Area (km^2)	Height (m)	Depth (m)
Mean	719	1168	1.58	0.96	183.2	2127.1
Median	463	710	1.44	0.26	124.6	2051.1
Standard deviation	759	1329	0.55	2.19	195.7	369.3
Minimum	125	125	1.0	0.02	3.3	1622.0
Maximum	6368	9732	4.31	21.71	1032.7	3160.7

nannofossils were identified; however evidence of reworking of early Eocene zones NP14a- NP12 nannofossils, *Discoaster kuepperi* and *Discoaster lodoensis*, was observed (Kevin Cooper, personal communication 2011).

Pelagic limestone

More indurated limestone (R1341-7) was pulled out of a bedrock outcrop (2914 m) on a 14° slope. Limestone (R1341-10) was collected from the top of a bedrock outcrop (2888 m) on a 30° slope. Microfossils *Globigerina* spp. and *Orbulina* spp. (Mid-Miocene to present) were found in both limestone samples (R1341-7 and R1341-10).

Bedded sedimentary rock covered with Fe–Mn oxide crusts

The most common type of bedrock observed on ROV dive R1343 was bedded sedimentary rock (**Figures 8A–C**), for example, as exposed on the SW and SE flanks of the second mound surveyed on that dive. Attempts to collect pieces of this bedrock yielded only the Fe–Mn oxide crusts, without the underlying bedrock. Therefore its age and composition remains unknown.

Biological Observations of Cold-Water Coral Distributions

Cold-water corals, including a variety of octocorals and three species of solitary scleractinian corals, were observed on the Orphan Knoll mounds, and on soft sediments between mounds. The coral morphotypes observed on the ROV dives are shown in **Figure 11**.

Figures 12A,B summarize the distribution of cold-water coral observations on dive R1341, and dive R1343, respectively. Contrary to expectations, coral morphotypes that normally require hard substrates were commonly observed in areas with dominantly fine sediment, but growing on isolated cobbles and boulders, presumably ice-rafted. Quantitative analysis of coral distributions in relation to surficial geology will be published separately.

One of the principal objectives of the Orphan Knoll cruise in 2010 was to collect sub-fossil solitary scleractinian corals, *D. dianthus*, from the coral graveyard discovered on the Northeast OK mounds in 1978. This coral graveyard was observed, and sampled again using the ROV during ROPOS dive R1343. The corals in this time-averaged accumulation were partially buried in mixed gravelly muddy sediment, in which the transported gravel component was polymictic, and sub-rounded to angular in shape. Some basalt samples were observed within the rock samples recovered. These basalt samples were subangular clasts within the sediment at the coral graveyard, co-occurring with granites, limestones, and other lithologies as well as the sub-fossil corals (**Supplementary Table 1**), and were most likely sourced from ice-rafted debris. The exposed portions of the coral skeletons were heavily encrusted with Fe–Mn oxides.

DISCUSSION

Mound Form, Distribution, and Probable Origin

Previous hypotheses for the origin of the mounds have been of two main types: those that emphasize the positive relief of the mounds and those that focus on the depressions around the mounds. In this contribution we attempt to interpret the mounds with horizontal dimensions of generally less than 1.5 km and elevations of less than 300 m that have been investigated in the 2017 *Discovery* multibeam data and the ROV dives. The large isolated mounds on southwestern Orphan Knoll, 2 km wide and 400 m high, were not investigated in this study and may have a quite different origin (Enachescu, 2004).

An early interpretation that involved the depressions between the mounds was the concept of a submerged karst plateau of Paleozoic limestone (Parson et al., 1984). This explanation predates modern seismic and multibeam sonar coverage and seems unlikely, given the thick Mesozoic–Cenozoic succession in the area of the mounds (**Figure 4**) and the resulting generally flat sea floor between the mounds (**Figure 5**). No submerged dolines or other clearly karst-related geomorphic features (e.g., Taviani et al., 2012) were observed in the seismic or multibeam data or in ROV observations. Small-scale depressions and possible erosional or dissolutional scour features are seen in layers 1 and 2 on the top of the NE Orphan Knoll mound (**Figures 8**, **9**, **12**). The depressions might have an origin in subaerial dissolution in the Cenomanian to Maastrichtian unconformity (Dafoe et al., 2017), similar to the dissolution of Cretaceous chalks of the Wyandot Formation on the Scotian Shelf (Wielens et al., 2002). Alternatively, depressions might result from submarine fluid escape (Land et al., 1995; Wielens et al., 2002). However, neither seismic profiles (**Figure 4**) nor the new multibeam bathymetry provide support for any of these interpretations.

The possibility of strong erosional bottom currents forming the observed curved depressions (**Figures 7B,C**) cannot be ruled out. The high-velocity core of the Deep Western Boundary Undercurrent (WBUC) is known to pass along the NE edge of Orphan Knoll. Current meter data from Orphan Knoll indicate that the Knoll as a whole induces a Taylor column, with cyclonic water circulation around the Knoll (Greenan et al., 2010). The small size of most of the mounds visible

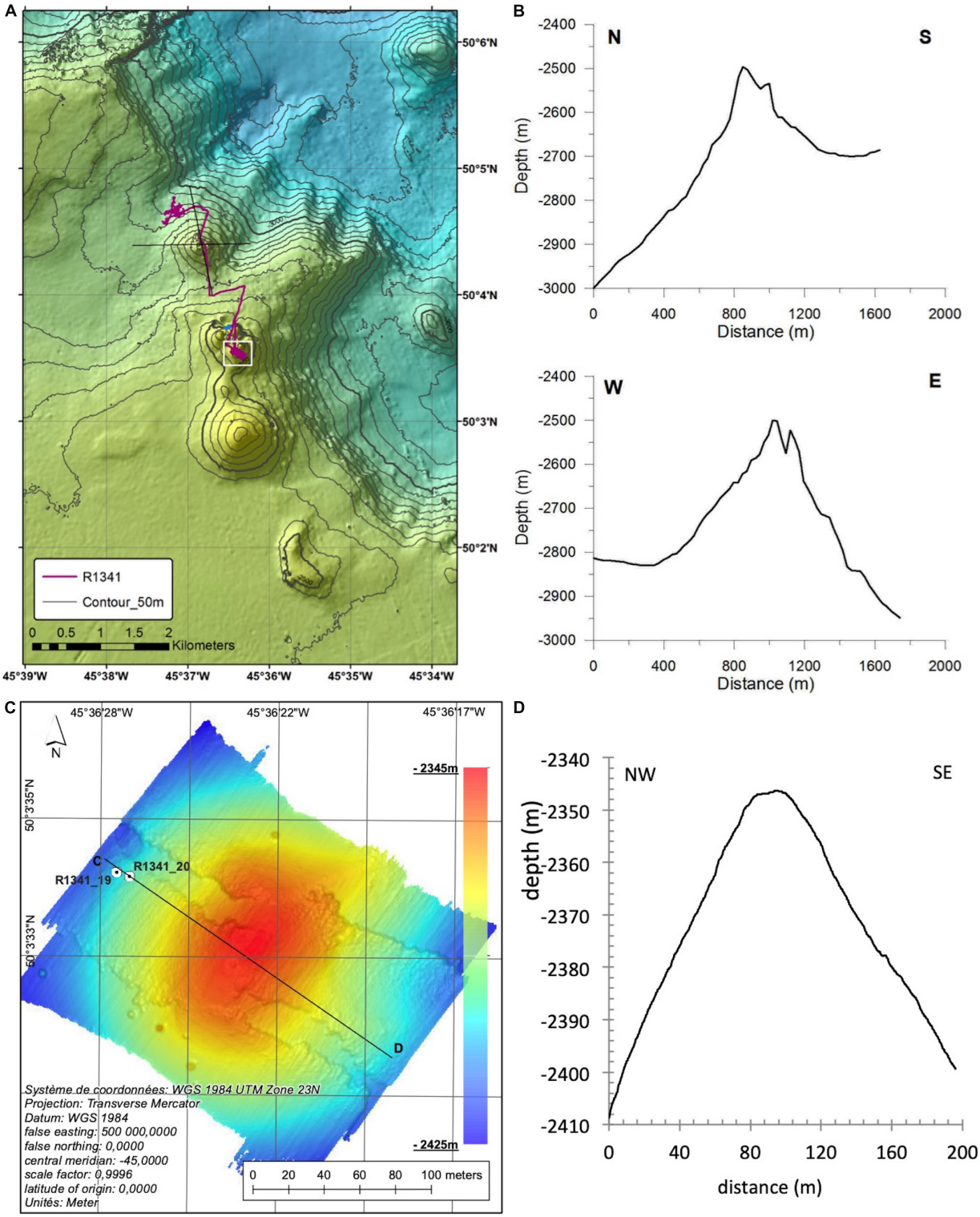

FIGURE 6 | Detailed bathymetry of mounds on the SE tongue of Orphan Knoll. **(A)** ICY_LAB multibeam sonar of mounds surveyed on ROPOS dive R1341. Multibeam sonar gridded to 26 m resolution. **(B)** Bathymetric profiles of the first mound encountered on dive R1341, based on 2017 ICY-LAB multibeam data. Full mound profiles are slightly concave, consistent with conical shape in 3D. **(C)** Near-bottom ROV-based bathymetry of SE Orphan Knoll mound mapped during ROV dive R1341, at 25 cm grid. The domal shape of the mound is evident despite the swath/navigation artifacts that we were unable to remove from the sonar data. These artifacts are likely related to the maximum 5 Hz navigation data available for ROV position. **(D)** Bathymetric profile C–D across mound, based on near-bottom ROV-based multibeam sonar parallel to multibeam acquisition swaths to minimize influence of position and swath artifacts.

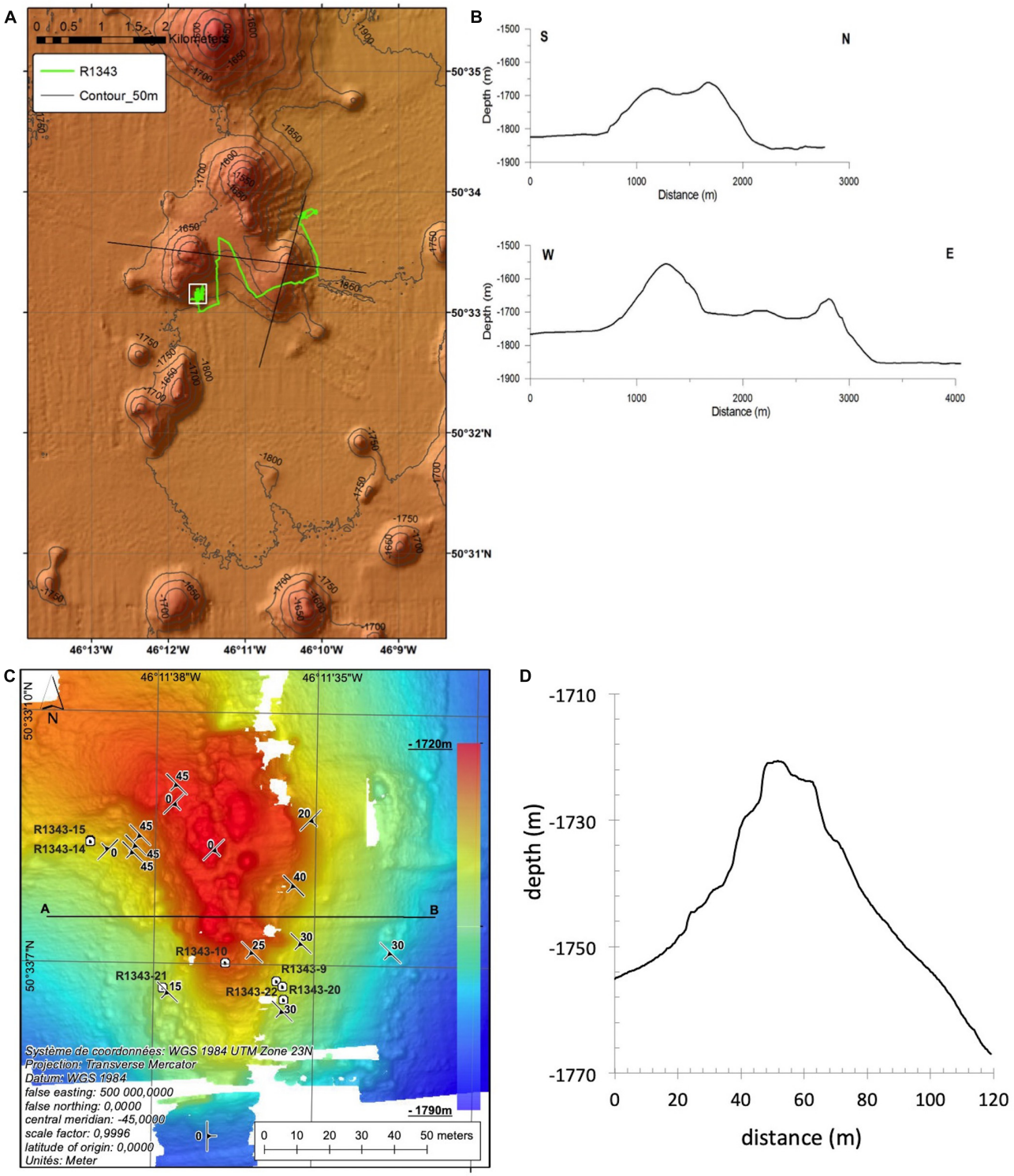

FIGURE 7 | Detailed bathymetry of the mound complex on NE Orphan Knoll, including the site of the coral graveyard collection. **(A)** ICY-LAB multibeam sonar of mounds,including mounds surveyed on ROPOS dive R1343. Multibeam bathymetry gridded to 25 m. **(B)** Bathymetric profiles across one (N–S) and two (W–E profile) mounds in 25 m grid bathymetry. The West-to East profile line crosses both mounds surveyed on dive R1343. VE = 2. **(C)** Detailed of bathymetry of the mound sampled in ROPOS dive R1343, also showing strike and dip measurements and locations of rock sample collections (see **Supplementary Table 1**). **(D)** Bathymetric profile A–B across ridge-shaped portion of mound surveyed with near-bottom multibeam sonar. VE = 2.

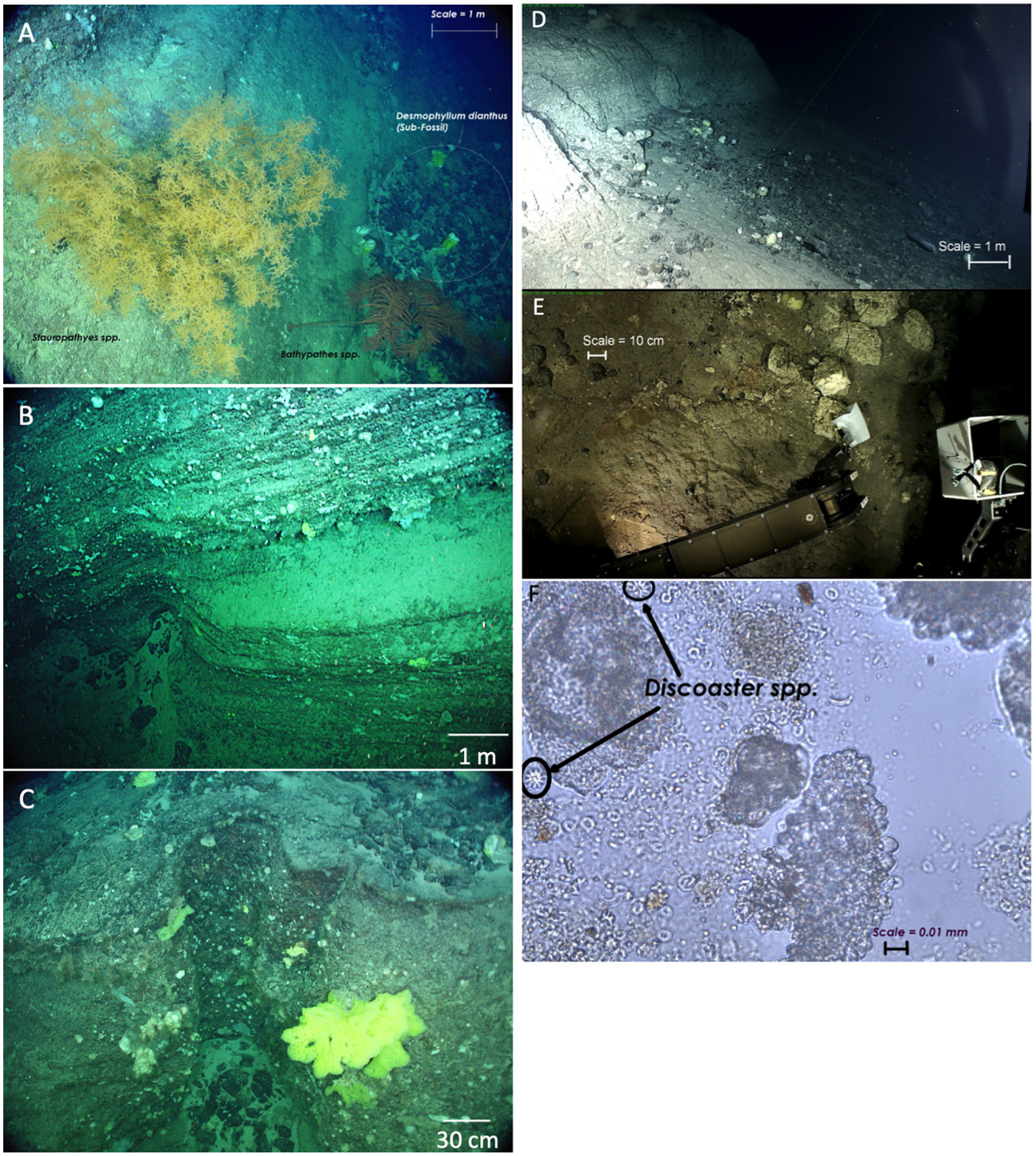

FIGURE 8 | Remotely operated vehicle bottom photos. **(A–C)** Bottom photos of stratified sedimentary bedrock at Orphan Knoll northeast mounds, ROV dive R1343. **(A)** View of bedrock wall above the coral graveyard collection site, with two large antipatharian corals growing on the wall. **(B)** Scour feature and bedded sedimentary rock along the base of the bedrock wall. **(C)** Another scour feature along the base of the bedrock wall. Scale bar for **(C)** is approximate, because laser pointers were on a curved portion of the bedrock wall. **(D–F)** ROV photos of calcareous ooze and polylmetallic nodules in segment A–A′ of ROV dive R1341. **(D)** Weakly indurated calcareous ooze outcrop. **(E)** Polymetallic nodules eroding form the calcareous ooze. Polymetallic nodules collected from this site were estimated as Eocene in age, based upon Re/Os dating (Poirier et al., 2011). **(F)** Smear microphotograph of calcareous ooze. Analysis of microfossils within the ooze suggested Eocene age. The ooze probably post-dates the indurated bedrock exposures observed on the other mounds of the southeast tongue of Orphan Knoll.

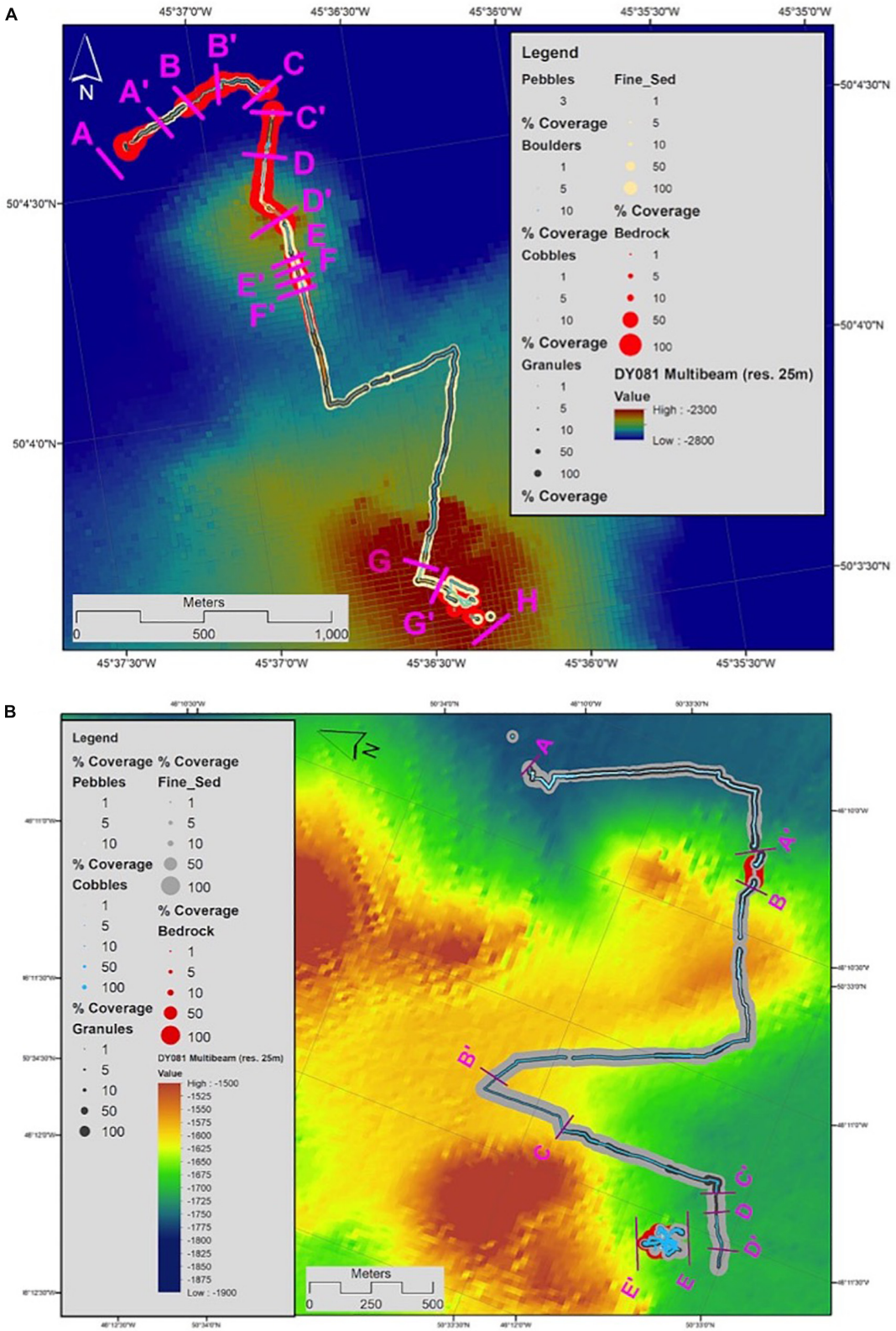

FIGURE 9 | Track of ROV dives, annotated for surficial geology. Bedrock exposure areas are indicated in red. **(A)** Dive R1341, SE Orphan Knoll. Bedrock areas were found most extensively in segments A–A′, B–C, C′–D′, and G′–H. **(B)** R1343, NE Orphan Knoll. Observations in **Figures 8**, **10** are from segment E–E′, which was the most carefully mapped segment of bedrock exposure, and was also the site of the subfossil coral graveyard.

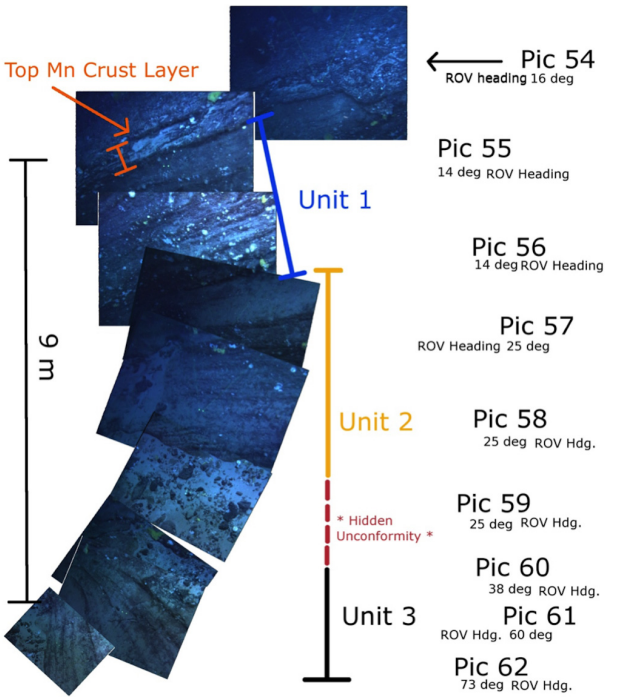

FIGURE 10 | Video frame grabs as ROPOS traveled down the exposed SW side of the NE OK mound in dive R1343. The picture ID is labeled 'Pic' and the heading of ROPOS is shown below the picture ID. Units 1 and 2 are of the same strike and dip; however Unit 2 has thicker bedded layers than Unit 1. Unit 3 is of a different strike than Units 1 and 2, and has no apparent dip. The summary of all strike and dip observations on the mound are presented in **Figure 7C**.

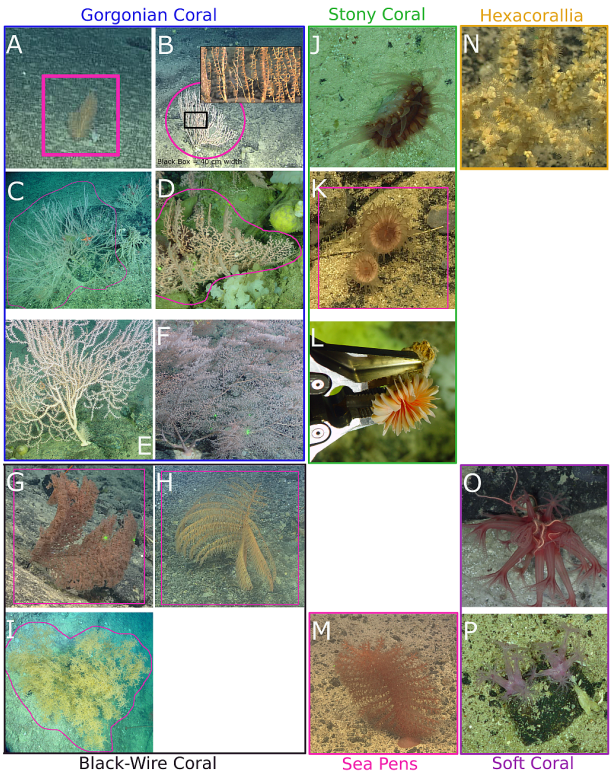

FIGURE 11 | Cold-water corals observed on the Orphan Seamount and Orphan Knoll. 'Gorgonian' corals: (top left): **(A)** *Acanella arbuscula*. **(B)** Isididae. **(C)** Keratoisidinae. **(D)** *Corallium* sp., probably *C. niobe* **(E)** *Paramuricea* sp. **(F)** *Chrysogorgia* sp. Black-wire coral (bottom-left): **(G)** Antipatharia indet., **(H)** *Bathypathes* sp., **(I)** *Stauropathes* sp., Stony coral (green box): **(J)** *Flabellum* sp., **(K)** *Caryophyllia ambrosia*, **(L)** *Desmophyllum dianthus*. Sea Pens (pink box): **(M)** various sea pen species, the most common was *Pennatula* spp., as shown here, Hexacorallia (top right): **(N)** Zoantharia, and Soft corals (bottom-right): **(O)** *Anthomastus* spp., **(P)** Nephtheidae. All corals identified visually, hence morphospecies, except for corals shown in **(C,D,F,H–L)**, for which voucher specimens were collected.

in the multibeam, however, suggests that the mounds are too small to have induced cyclonic currents surrounding them from small Taylor columns. They may, however, experience inertial currents moving around the mounds, perhaps under the influence of unusually strong winter storms (cf. Li et al., 2017). Variations in sediment accumulation rates in piston cores from Orphan Knoll (Piper, unpublished data) suggest that there are local effects of near-bottom currents. Bottom currents were likely stronger in the Holocene than in the glacial Pleistocene (Mao et al., 2018). The very thin Miocene section in DSDP 111 suggests particularly erosional bottom water conditions as the Oligocene-Mid Miocene abyssal circulation changed in the western North Atlantic Ocean (Miller and Fairbanks, 1983). The ROV observations and samples of bedrock mostly indicated thinly bedded to massive sedimentary rock with extensive Fe–Mn encrustation, suggesting a long duration of submarine exposure. Corals collected from the coral graveyard at R1343 included samples as old as 181 ka, from Marine Isotope Stage (MIS) 7 (Ménabréaz et al., 2015; Maccali et al., in review). Osmium isotope studies of the polymetallic nodules from R1341 suggested an Eocene origin, with a hiatus in accretion during the Miocene (Poirier et al., 2011). Geochemical evidence on the subfossil corals collected from the graveyard site at R1343 suggests that the corals were buried and later exhumed by Holocene current scour (Maccali et al., in review). Strong Holocene current winnowing of hemipelagic sediments from the corals in the coral graveyard are suggested as a taphonomic mechanism causing degradation of the coral samples, and perhaps concentration of the coral samples by removal of intervening fine sediments. Such current winnowing would also help explain the abundance of polymictic gravels containing Paleozoic limestone derived from Arctic Canada within the coral graveyard deposit, consistent with ice-rafted debris supplied during Heinrich events. The bottom type observations during ROV dives R1341 and R1343 found sloping areas of mud and mixed lithic clasts surrounding the exposed bedrock core of mounds. These apparent hemipelagic sediments could be affected by current winnowing and sediment drift, but no diagnostic features were observed. We therefore conclude that locally in the Holocene and perhaps during other full interglacials near bottom currents were strong enough to modify the sea floor. On the other hand, clear current scour moats or other features typically associated with prolonged formation of contourite drifts (van Rooij et al., 2007; Esentia et al., 2018) were

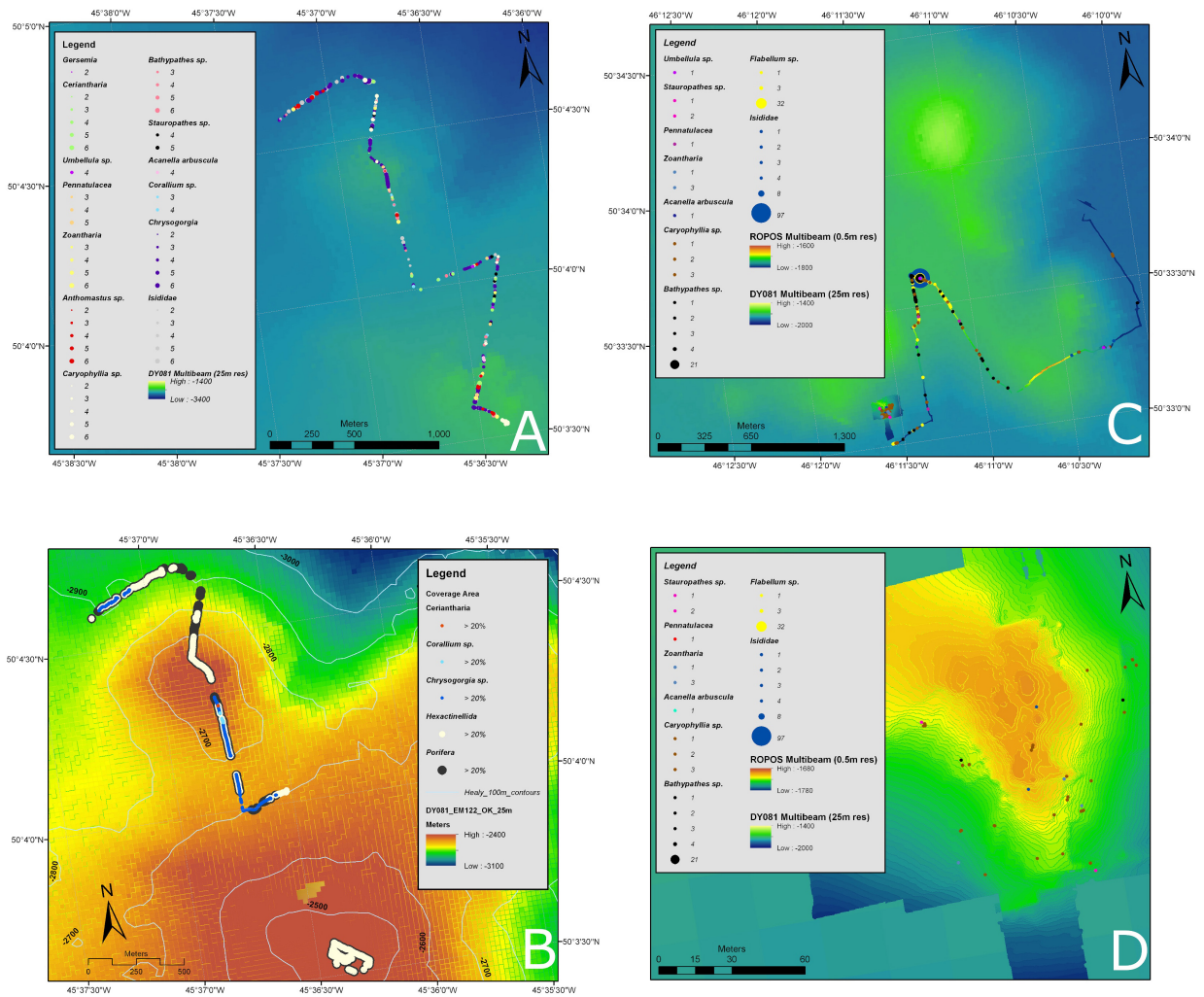

FIGURE 12 | Distribution of cold-water coral observations along ROPOS dives. **(A,B)** Coral observations on SE Orphan Knoll dive R1341. **(A)** Coral observations. **(B)** Locations of faunal concentrations of corals and sponges > 20% cover. See **Figure 9A** for surficial geology layer. **(C,D)** Coral observations on NE Orphan Knoll dive R1343. **(C)** Coral distributions throughout dive R1343. See **Figure 9B** for the surficial geology layer. The track of the ROV showing coral occurrences is overlaid over DY081 bathymetry. Coral abundances not adjusted for area observed. White box indicates location of **(D)**. **(D)** Coral observations surrounding bedrock outcrop mapped in **Figure 8C**, including *Desmophyllum dianthus* coral graveyard. See **Figure 9B** for surficial geology layer, and see **Figure 7C** for underlying ROV-derived bathymetry below **(D)**.

not observed around any of the mounds in the 2017 *Discovery* multibeam data (**Figure 5**), nor in seismic profiles (**Figure 4**).

A striking morphological features of the mounds revealed in the 2017 Discovery multibeam data is their approximately conical shape. This morphology is superficially similar to the shape of subaerial cinder cones or submarine volcanic seamounts (Casalbore, 2018), though at a smaller than normal scale than seamounts as usually defined (e.g., Harris et al., 2014). A volcanic origin can be excluded based on the seismic profiles through the mounds (**Figure 4**), complete lack of evidence in ROV observations and the lack of magnetic anomaly detected in several magnetometer surveys across the Knoll, starting with the 1969 Charcot survey, and magnetometer surveys associated with the DSDP expedition (Laughton et al., 1972).

Visual observations using the ROV likewise uncovered no evidence for a biogenic origin of the mounds, i.e., cold-water coral carbonate mounds (Huvenne et al., 2003; Roberts et al., 2006). The mounds were clearly colonized by cold-water corals, mostly octocorals, with a few antipatharians, and by sponges, but the mounds were not composed of coral skeletons. Stratified late Pleistocene sediment imaged by seismic profile on a mound crest (**Figure 4A**) is inconsistent with a biogenic mound origin. Our lack of observation of biogenic mounds does not preclude the presence of biogenic mounds, formed by corals or sponges, elsewhere on the Orphan Knoll or adjacent regions such as the Sackville Spur (Campbell, personal communication). Nor does it preclude the possibility of buried biogenic mounds of pre-mid Quaternary age forming a substrate for proglacial hemipelagic deposition in the later Quaternary.

One of the early proposed origins of the mounds on Orphan Knoll was the presence of (aligned) bedrock ridges. Laughton et al. (1972) proposed apparently aligned mounds, but on the basis of single-beam sonar data on hand-drawn maps. Higher resolution seismic profiles (**Figure 4C**) show faulting of Mesozoic-Cenozoic bedrock, with some faults extending upwards to near the seabed. The 2017 *Discovery* mapping of the mounds on NE Orphan Knoll shows local alignment of series of several mounds, for example ESE–WNW at 50°40′ N near the eastern edge of the Knoll, and almost N–S at around 50°30′ N (**Figure 5D**), extending northward to the mounds in **Figure 4A**. Thus although the overall data shows no statistical preferred orientation, the patterns of mound distribution are consistent with alignment along relatively short fault segments (<5 km in length).

Bedrock orientation observed from dive R1343, with generally westward to southwestward dip angles, is consistent with the concept that mounds are fault bounded and experienced some tilting. So too are the gentle dips in fault-bound blocks of Cenozoic-Quaternary strata visible in seismic profiles (**Figure 4C**). The seismic profiles suggest that some of the mounds could expose Mesozoic strata at their base. The Eocene age of the calcareous ooze sampled at the beginning of dive R1341 is consistent with this interpretation. The Quaternary section over the mounds appears condensed compared with that in flat areas of the crest of Orphan Knoll (**Figure 4**), not unexpected given the regional southward flowing currents (Hall et al., 2013).

With available data, it is difficult to further characterize the faulting style. They may represent normal, possibly listric faults, structurally similar to the extensional faulting within the Orphan Basin (Dafoe et al., 2017). Alternatively, the faults may be parallel to the NNW-trending fault-bound northeastern face of Orphan Knoll, although this is not supported by orientations of groups of mounds in the bathymetry (**Figure 5D**). Quaternary neotectonic faulting has been demonstrated farther south on Flemish Cap (Normandeau et al., 2019) but is not apparent in Orphan Basin.

The available data suggest that the short linear groups of mounds represent tilted fault blocks of uplifted Mesozoic-Cenozoic bedrock on Orphan Knoll. A highly condensed section in Oligocene and Miocene pelagic sediments with hiatuses was intersected by DSDP 111 and the seismic signature is irregular, suggestive of bottom current winnowing. At that time, fault uplift may have exceeded burial by accumulated sediment, and the resulting fault scarps would have been susceptible to mass wasting, similar to that seen at the seabed today on the NE face of Orphan Knoll. Localized submarine landsliding and winnowing by bottom currents broke up the short fault scarps into a series of residual erosional highs, as evidenced by the Eocene sediment recovered on dive 1341. With increased sediment supply in the Pliocene and particularly the Quaternary, this erosional landscape was blanketed by distal proglacial hemipelagic sediment. Sculpting of this hemipelagic sediment by bottom currents, particularly when sedimentation rates were a little lower in the early Pleistocene and Pliocene, probably contributed to mound morphology, as sediment was swept off the crests of the mounds and accumulated on the flanks, and small landslides also developed on the steep flanks.

Despite a long but scattered history of study, ROV observations and rock collections, and an extensive new multibeam dataset, the origin and composition of the enigmatic Orphan Knoll mounds remains unclear. The hypothesis of a fault-based origin of the mounds is supported, but not confirmed, by the data in this study. The juxtaposition of the new multibeam data demonstrating approximately conical shape and no strong systematic alignment of mounds, with the ROV observations suggesting block-faulted sedimentary bedrock composition for at least one of the mounds observed, serves to reinforce the necessity of sub-bottom or seismic data, *in situ* direct observations, and ROV-based bedrock collections, to complement interpretations of seafloor mounds origins based on mound shape revealed in remotely sensed bathymetry. It is possible that a 1–2 days of dedicated high-resolution deep-towed seismic surveys around some of the larger and more isolated mounds could detect faults surrounding more of the mounds on Orphan Knoll.

Significance of Biological Observations, Particularly Deep-Sea Corals

The coral fauna observed on Orphan Knoll was generally similar to the fauna observed elsewhere in the Newfoundland and Labrador region, with the exception of two species. First, the gorgonian coral, *Corallium? niobe*, was observed on the SE Orphan Knoll mounds (R1341). Further samples of *C. niobe* were collected during the DY081 cruise ROV dives on Orphan Knoll in 2017 (Hendry, 2017).

The small-scale distribution of hard-substrate dependent species on the Orphan Knoll was not limited to mound bedrock. All types of hard-substrate dependent corals and sponges were also observed growing on ice-rafted debris, on clasts ranging in size from small cobbles to large boulders (Meredyk, 2017). The abundant ice-rafted debris in the Northwest Atlantic may weaken apparent substrate limitations for cold-water coral species that require hard-substrate attachment surfaces (Miles, 2018).

The solitary scleractinian coral *Caryophyllia ambrosia* was observed in muddy sediments between the mounds on Orphan Knoll, on dives R1345 and R1346. While this species is well-known from deep-water environments elsewhere, it has not previously been recorded in the Newfoundand and Labrador region.

Overall our data suggest that the mounds were not built by scleractinian corals, as has been reported for mounds in the Porcupine Seabight or Rockall Trough, for example (NE Atlantic, Mienis et al., 2006; Kano et al., 2007), nor authigenic carbonates colonized by cold-water corals. Although evidence was found for moderate densities of *D. dianthus* in some locations, the mounds were also not covered by extensive scleractinian reefs, which was one of the underlying hypotheses that supported the 2008 NAFO decision to close the area to bottom-contact fisheries. However, the evidence provided here shows that the hard substratum and habitat complexity provided by the mounds support a diverse fauna that includes a large number of other cold-water coral and benthic species, which are protected from fisheries impacts by the NAFO closure. Independent of their origin and development mechanism, deep-sea mounds often

provide an attractive environment for benthic communities that warrant conservation.

CONCLUSION

The 'Enigmatic Mounds' on Orphan Knoll remain enigmatic. The majority of mounds surveyed to date are less than 1 km^2 in area and < 100 m in height above the surrounding portions of Orphan Knoll. The mounds surveyed in new multibeam data are mostly conical in form, without a clear preferred orientation or apparent alignment.

Remotely operated vehicle observations of the Orphan Knoll mounds including near-bottom ROV-based multibeam surveys suggested domal to ridge-shaped mounds, some with potential collapse features around some edges. The *in situ* camera observations on one mound suggested that the mound bedrock was composed of bedded sedimentary rock, probably siliciclastic, with a prevailing, but not uniform, dip direction to the southwest. These observations are consistent with a block-faulted origin of the observed mounds. No direct evidence of former subaerial processes, submarine volcanic rocks, mud-volcanoes, karst dissolution, or cold-water coral bioherms was observed.

Our results emphasize the importance of *in situ* observations and rock sample collections to complement remotely-sensed bathymetric datasets, and the need for improved techniques of ROV-based submarine bedrock collection and submarine bedrock structural analysis.

DATA AVAILABILITY STATEMENT

The *USCGC Healy* and *Kommandor Jack* multibeam sonar and Geological Survey of Canada seismic data are available through the Canadian Hydrographic Service and the Geological Survey of Canada, but with some confidentiality limitations applied to the *Kommandor Jack* data compiled for the Canadian UNCLOS claim. The UNCLOS Atlantic Ocean multibeam data reside with CHS and are available through a request sent to: CHS ATL Data Centre/Centre de Données CHS ATL. DFO.CHSATLDataCentre-CentreDeDonneesCHSATL.MPO@dfo-mpo.gc.ca. HUDSON 2010-029 mission data and ROPOS multibeam data are archived at the Geological Survey of Canada and at Memorial University, and are available upon request from the authors. The ICY-LAB multibeam bathymetry data are archived at the National Oceanography Centre, Southampton, United Kingdom. ICY-LAB EM-122 multibeam swath bathymetry datasets are now published on PANGAEA (doi: 10.1594/PANGAEA.892825) and are free to access.

AUTHOR CONTRIBUTIONS

SM compiled the archival multibeam, side-scan, and sub-bottom profile data, participated in the field work aboard *CCGS Hudson* Cruise 2010-029, processed the video, identified the rock samples, identified the corals and sponges in video, and contributed to the writing. EE and DP directed the thesis of SM. EE participated in the field work aboard *CCGS Hudson* cruise 2010-029, guided the interpretations, and contributed to the writing. DP provided archival multibeam, side-scan, and sub-bottom profile data, guided the interpretations, and contributed to the writing. VH and SH collected, processed, and analyzed the multibeam sonar data on cruise DY081, and contributed to the writing. AR guided the interpretations and contributed to the writing, particularly with detailing the history of geological exploration and mapping of Orphan Knoll.

FUNDING

This research was supported by NSERC Discovery Grants to EE and DP. *CCGS Hudson* ship-time and ROV support was funded by an NSERC ship time grant to EE and co-applicants, and by Fisheries and Oceans Canada (DFO) International Governance Strategy (IGS) grants to K. Gilkinson and E. Kenchington, and DFO ship time allocated to E. Kenchington. Support for SM studies was provided by funding from the Memorial University, NSERC Discovery Grants to EE and DP, and the Geological Survey of Canada. 2017 ship time aboard *RRS Discovery* was funded by a NERC (United Kingdom) ship-time grant to ICY-LAB Principal Investigator Kate Hendry. Additional support was received from a Memorial University 2018-19 sabbatical research grant to EE and by European Research Council Starting grant # 678371.

ACKNOWLEDGMENTS

The authors would like to thank the captain and crew of *CCGS Hudson* and the Canadian Scientific Submersible Facility (CSSF) ROV team, for support during the *Hudson* 2010-029 mission. The authors would also like to thank the Principal Investigator Kate Hendry, together with the captain, crew, and scientific party of the ICY-LAB expedition DY081. R. Devillers (MUN) guided the collection and processing of near-bottom multibeam data during and after *CCGS Hudson* 2010-029 cruise. S. Bermell (IFREMER) reprocessed the near-bottom multibeam rasters to highlight geomorphic features, and generated high-resolution bathymetric profiles of two mounds. This manuscript was completed while EE was on sabbatical leave at IFREMER Centre Bretagne, France. EE thanks IFREMER for cartographic and computational support. Dedicated to the memories of Edgar Edinger (1919–2018), Anthony Laughton (1927–2019), Jan E. van Hinte (1935–2019), and Callum Mireault (1991–2018).

SUPPLEMENTARY MATERIAL

The Supplementary Material for this article can be found online at: https://www.frontiersin.org/articles/10.3389/fmars.2019.00744/full#supplementary-material

REFERENCES

Barrett, T. J., Jarvis, I., Longstaffe, F. J., and Farquhar, R. (1988). Geochemical aspects of hydrothermal sediments in the eastern Pacific Ocean; an update. *Can. Mineral.* 26, 841–858.

Blénet, A. (2016). *La Taphonomie des Coraux Profonds des Cimetirères sous-marins d'Orphan Knoll et de Flemish Cap, Une Étude Préliminaire aux Analyses Géochimiques*. M.Sc. thesis, Université du Québec à Montréal, Montreal.

Bolton, B. R., Both, R., Exon, N. F., Hamilton, T. F., Ostwald, J., and Smith, J. D. (1988). Geochemistry and mineralogy of seafloor hydrothermal and hydrogenetic Mn oxide deposits from the Manus Basin and Bismarck Archipelago region of the southwest Pacific Ocean. *Mar. Geol.* 85, 65–87. doi: 10.1016/0025-3227(88)90084-9

British Admiralty (1917). *North Atlantic Ocean, Eastern Portion*. London: British Admiralty.

Burton-Ferguson, R., Enachescu, M. E., and Hiscott, R. (2006). *Preliminary seismic interpretation and maps for the Paleogene-Neogene (Tertiary) Succession, Orphan Basin* (Canada: Memorial University of Newfoundland), 28–32.

Casalbore, D. (2018). "Volcanic islands and seamounts," in *Submarine Geomorphology*, eds A. Micallef, S. Krastel, and A. Savini, (Berlin: Springer), 333–347. doi: 10.1007/978-3-319-57852-1_17

Ceramicola, S., Dupre, S., Somoza, L., and Woodside, J. (2018). "Cold seep systems," in *Submarine Geomorphology*, eds A. Micallef, S. Krastel, A. Savini, (Berlin: Springer), 367–387. doi: 10.1007/978-3-319-57852-1_19

Channell, J. E. T., Hodell, D. A., Romero, O., Hillaire-Marcel, C., De Vernal, A., Stoner, J. S., et al. (2012). A 750-kyr detrital-layer stratigraphy for the North Atlantic (IODP Sites U1302–U1303. Orphan Knoll, Labrador Sea). *Earth Planet. Sci. Lett.* 317, 218–230. doi: 10.1016/j.epsl.2011.11.029

Chian, D., Reid, I. D., and Jackson, H. R. (2001). Crustal structure beneath Orphan Basin and implications for nonvolcanic continental rifting. *J. Geophys. Res.* 106, 923–940.

Conway, K., Barrie, J. V., and Krautter, M. (2005). Geomorphology of unique reefs on the western Canadian shelf: sponge reefs mapped by multibeam bathymetry. *Geol. Mar. Lett.* 25, 205–213. doi: 10.1007/s00367-004-0204-z

Cormier, M.-H., and Sloan, H. (2018). "Abyssal hills and abyssal plains," in *Submarine Geomorphology*, eds A. Micallef, S. Krastel, and A. Savini, (Berlin: Springer), 389–408. doi: 10.1007/978-3-319-57852-1_20

Dafoe, L. T., Keen, C. E., Dickie, K., and Williams, G. L. (2017). Regional stratigraphy and subsidence of Orphan Basin near the time of breakup and implications for rifting processes. *Basin Res.* 29, 233–254. doi: 10.1111/bre.12147

Deutschen Hydrographischen Institut (1964). *General Bathymetric Chart of the Oceans (GEBCO), Deut. Hydro*. Hamburg: Deutschen Hydrographischen Institut.

Dronov, A. (1993). Middle paleozoic waulsortian-type mud mounds in Southern Fergana (Southern Tien-Shan, commonwealth of independent states): the shallow-water atoll model. *Facies* 28, 169–180. doi: 10.1007/bf02539735

Edinger, E. N., and Sherwood, O. A. (2012). Applied taphonomy of gorgonian and antipatharian corals in Atlantic Canada: experimental decay rates, field observations, and implications for assessing fisheries damage to deep-sea coral habitats. *Neues Jahrb. Geol. Paläontol.* 265, 199–218. doi: 10.1127/0077-7749/2012/0255

Enachescu, M., Kearsey, S., Hardy, V., Sibuet, J.-C., Hogg, J., Srivastava, S., et al. (2005). "Evolution and petroleum potential of Orphan Basin, offshore Newfoundland, and its relation to the movement and rotation of Flemish Cap based on plate kinematics of the North Atlantic," in *Petroleum Systems of Divergent Continental Margin Basins*, eds N. Rosen, D. Olsen, S. L. Palmes, K. T. Lyons, and G. B. Newton, (Houston, TX: GCSSEPM), 75–131. doi: 10.5724/gcs.05.25.0075

Enachescu, M. E. (2004). Conspicuous deepwater submarine mounds in the northeastern Orphan Basin and on the Orphan Knoll, offshore Newfoundland. *Lead. Edge* 23, 1290–1294. doi: 10.1190/leedff.23.1290_1

Esentia, I., Stow, D., and Smillie, Z. (2018). "Contourite drifts and associated bedforms," in *Submarine Geomorphology*, eds A. Micallef, S. Krastel, and A. Savini, (Berlin: Springer), 301–331. doi: 10.1007/978-3-319-57852-1_16

Forsterra, G., Beuck, L., Häussermann, V., and Freiwald, A. (2005). "Shallow-water *Desmophyllum dianthus* (Scleractinia) from Chile: characteristics of the biocoenoses, the bioeroding community, heterotrophic interactions and (paleo)-bathymetric implications," in *Cold-Water Corals and Ecosystems. Erlangen Earth Conference Series*, eds A. Freiwald, and J. M. Roberts, (Berlin: Springer), 937–977. doi: 10.1007/3-540-27673-4_48

Greenan, B. J. W., Yashayaev, I., Head, E. J. H., Harrison, W. G., Azetsu-Scott, K., Li, W. K. W., et al. (2010). *Interdisciplinary Oceanographic Observations of Orphan Knoll*. Dartmouth: Northwest Atlantic Fisheries Organization.

Hall, M. M., Torres, D. J., and Yashayaev, I. (2013). Absolute velocity along the AR7W section in the Labrador Sea. *Deep Sea Res.* 72, 72–87. doi: 10.1016/j.dsr.2012.11.005

Harris, T., Macmillan-Lawler, M., Rupp, J., and Baker, E. K. (2014). Geomorphology of the Oceans. *Mar. Geol.* 352, 4–24. doi: 10.1016/j.margeo.2014.01.011

Hart, B. (1977). The mid-Cretaceous succession of Orphan Knoll (northwest Atlantic): micropaleontology and palaeo-oceanographic implications. *Deep Sea Res.* 24, 272–272.

Hendry, K. (2017). *RRS Discovery Cruise DY081 cruise report: ICY-LAB (Isotope sampling in the Labrador Sea)*. Fort Lauderdale, FL: National Marine Facilities.

Henriet, J., Hamoumi, N., Da Silva, A. C., Foubert, A., Lauridsen, B. W., Ruggeberg, A., et al. (2014). Carbonate mounds: from paradox to World Heritage. *Mar. Geol.* 352, 89–110. doi: 10.1016/j.margeo.2014.01.008

Henriet, J., Spezzaferri, S., Samankassou, E., Foubert, A., van Rooij, D., and Ruggeberg, A. (2011). Carbonate mounds in shallow and deep time. *Mar. Geol.* 282, 1–4. doi: 10.1016/j.margeo.2011.02.010

Hiscott, R. N., Aksu, A. E., and Nielsen, O. B. (1989). Provenance and dispersal patterns, Pliocene-Pleistocene section at site 645, Baffin Bay. *Proc. Ocean Drill. Prog. Sci. Results* 105, 31–52.

Hovland, M., Croker, P. F., and Martin, M. (1994). Fault-associated seabed mounds(carbonate knolls?) off western Ireland and north-west Australia. *Mar. Pet. Geol.* 11, 232–246. doi: 10.1016/0264-8172(94)90099-x

Howell, K.-L., Piechaud, N., Downie, A.-L., and Kenny, A. (2016). The distribution of deep-sea sponge aggregations in the North Atlantic and implications for their effective spatial management. *Deep Sea Res.* 115, 309–320. doi: 10.1016/j.dsr.2016.07.005

Hoy, S. K., Hendry, K. R., and Huvenne, V. A. I. (2018). *North Atlantic EM-122 Multibeam Swath Bathymetry Collected During RRS Discovery Cruise DY081 (Links to Raw Files and Gridded Data)*. Los Angeles: PANGAEA.

Huvenne, V. A. I., de Mol, B., and Henriet, J. (2003). A 3D seismic study of the morphology and spatial distribution of buried coral banks in the Porcupine Basin, SW of Ireland. *Mar. Geol.* 198, 5–25. doi: 10.1016/s0025-3227(03)00092-6

Immenhauser, A., and Rameil, N. (2011). Interpretation of ancient epikarst features in carbonate successions — A note of caution. *Sediment. Geol.* 239, 1–9. doi: 10.1016/j.sedgeo.2011.05.006

Kano, A., Ferdelman, T. G., Williams, T., Henriet, J., Ishikawa, T., Kawagoe, N., et al. (2007). Age constraints on the origin and growth history of a deep-water coral mound in the northeast Atlantic drilled during integrated ocean drilling program expedition 307. *Geology* 35, 1051–1054.

Keen, C. E. (1978). *Cruise Report C.S.S.* Hudson: Bedford Institute of Oceanography.

Kenchington, E., Best, M., Cogswell, A., MacIsaac, K., Murillo-Perez, F. J., MacDonald, B., et al. (2009). *Accurate Identification of Deep-Water Coral Harvested in the NAFO Regulatory Area*. Dartmouth: Northwest Atlantic Fisheries Organization.

Land, L., Paull, C., and Hobson, B. (1995). Genesis of a submarine sinkhole without subaerial exposure: Straits of Florida. *Geology* 23, 949–951.

Laughton, A. S., Berggren, W. A., Benson, R. N., Davies, T. A., Franz, U., Musich, L. F., et al. (1972). *Site 111, Initial Reports of the Deep-Sea Drilling Project* (Washington, DC: U. S. Government Printing Office), 133–159.

Lecours, V., Gabor, L., Edinger, E., and Devillers, R. (2019). "Fine-scale cold-water coral habitat characterization of The Gully, the Flemish Cap and the Orphan Knoll, Northwest Atlantic," in *GEOHAB Atlas: Seafloor Geomorphology as Benthic Habitat, 2nd Edition*, eds T. Harris, and E. K. Baker, (Amsterdam: Elsevier).

Legault, J. (1982). First report of Ordovician (Caradoc-Ashgill) palynomorphs from Orphan Knoll, Labrador Sea. *Can. J. Earth Sci.* 19, 1851–1856. doi: 10.1139/e82-163

Li, M. Z., Wu, Y., Han, G., Prescott, R. H., and Tang, C. C. L. (2017). A modeling study of the impact of major storms on seabed shear stress and sediment transport on the Grand Banks of Newfoundland. *J. Geophys. Res.* 122, 4183–4216. doi: 10.1002/2016JC012215

Lo Iacono, C., Savini, A., and Basso, D. (2018). "Cold-water carbonate bioconstructions," in *Submarine Geomorphology*, eds A. Micallef, S. Krastel, A. Savini, (Berlin: Springer), 425–455. doi: 10.1007/978-3-319-57852-1_22

Maccali, J., Hillaire-Marcel, C., Ghaleb, B., Menabreaz, L., Blenet, A., Edinger, E., et al. (in review). Quaternary sporadic development of *Desmophyllum dianthus* deep-sea coral populations in the southern Labrador Sea with specific attention to their ^{14}C and ^{230}Th-dating. *Mar. Chem.*

Mao, L., Piper, D. J., Saint-Ange, F., and Andrews, J. T. (2018). Labrador Current fluctuation during the last glacial cycle. *Mar. Geol.* 395, 234–246. doi: 10.1016/j.margeo.2017.10.012

Mazzini, A., and Etiope, G. (2017). Mud volcanism: an updated review. *Earth Sci. Rev.* 168, 81–112. doi: 10.1016/j.earscirev.2017.03.001

Ménabréaz, L., Maccali, J., Blénet, A., Ghaleb, B., Poirier, A., Edinger, E., et al. (2015). *Neodymium Isotopic Composition of Deep-Sea Corals from the Labrador Sea: Implications for NW Atlantic Deep-Water Masses Circulation During the Holocene, MIS 5 and 7*. Montreal: AGU.

Meredyk, S. (2017). *Physical characterization and benthic megafauna distribution and species composition on Orphan Knoll and Orphan Seamount, NW Atlantic*. M.Sc. thesis, Memorial University of Newfoundland, Canada.

Mienis, F., van Weering, T., de Haas, H., de Stigter, H., Huvenne, V., and Wheeler, A. (2006). Carbonate mound development at the SW Rockall Trough margin based on high resolution TOBI and seismic recording. *Mar. Geol.* 233, 1–19. doi: 10.1016/j.margeo.2006.08.003

Miles, L. L. (2018). *Cold-Water Coral Distribution and Surficial Geology on the Flemish Cap, Northwest Atlantic*. M.Sc. thesis, Memorial University of Newfoundland, Canada.

Miller, K. G., and Fairbanks, R. G. (1983). Evidence for Oligocene–middle miocene abyssal circulation changes in the western North Atlantic. *Nature* 306:250. doi: 10.1038/306250a0

Moscardelli, L., Ramnarine, S. K., Wood, L., and Dunlap, D. B. (2013). Seismic geomorphological analysis and hydrocarbon potential of the lower cretaceous Cromer Knoll Group, Heidrun field, Norway. *AAPG Bull.* 97, 1227–1248. doi: 10.1306/02081312155

Normandeau, A., Piper, D. J. W., Shaw, J., Todd, B. J., Campbell, D. C., and Mosher, D. C. (2019). "Chapter 20: the seafloor of Southeastern Canada," in *Landscapes and Landforms of Eastern Canada*, eds O. Slaymaker, and N. Catto, (Berlin: Springer).

Parson, L. M., Masson, D. G., Pelton, C. D., and Grant, A. C. (1985). Seismic stratigraphy and structure of the east Canadian continental margin between 41 and 52° N. *Can. J. Earth Sci.* 22, 686–703. doi: 10.1139/e85-075

Parson, L. M., Masson, D. G., Rothwell, R. G., and Grant, A. C. (1984). Remnants of a submerged pre-Jurassic (Devonian?) landscape on Orphan Knoll, offshore eastern Canada. *Can. J. Earth Sci.* 21, 61–66. doi: 10.1139/e84-007

Pe-Piper, G., Meredyk, S., Zhang, Y., Piper, D. J. W., and Edinger, E. N. (2013). Petrology and tectonic significance of seamounts within transitional crust east of Orphan Knoll, offshore eastern Canada. *Geo-Mar. Lett.* 33, 433–447. doi: 10.1007/s00367-013-0342-2

Pe-Piper, G., Meredyk, S., Zhang, Y., Piper, D. J. W., and Edinger, E. N. (2014). Erratum to: petrology and tectonic signficance of seamounts within transitional crust east of Orphan Knoll, offshore eastern Canada. *Geo-Mar. Lett.* 34, 567–568.

Poirier, A., Hillaire-Marcel, C., Meredyk, S., and Edinger, E. (2011). Osmium isotopes in manganese nodules from the Labrador Sea. *Mineral. Mag.* 75:1653.

Riding, R., and Awramik, S. M. (2000). *Microbial Sediments*. Berlin: Springer.

Roberts, M., Long, D., Wilson, J. B., Mortensen, B., and Gage, J. D. (2003). The cold-water coral *Lophelia pertusa* (Scleractinia) and enigmatic seabed mounds along the north-east Atlantic margin: are they related? *Mar. Pollut. Bull.* 46, 7–20. doi: 10.1016/s0025-326x(02)00259-x

Roberts, M., Wheeler, A., and Freiwald, A. (2006). Reefs of the deep: the biology and geology of cold-water coral ecosystems. *Science* 312, 543–547. doi: 10.1126/science.1119861

Ruffman, A. (1971). *A Report on the Participation of A. Ruffman on the USNS LYNCH Cruise 7/11/71 in the North Atlantic*. Bedford Institute of Oceanography.

Ruffman, A. (2011). *Orphan Knoll as a Window on the Palaeozoic; Seemingly Ignored by the Petroleum Industry for 40 Years*. Calgary: Canadian Society of Petroleum Geology.

Ruffman, A., and van Hinte, J. E. (1973). "Orphan Knoll - A 'Chip' off the North American 'Plate'," in *Earth Science Symposium on Offshore Eastern Canada*, ed. J. Hood, (Ottawa: Geological Survey of Canada), 407–449.

Ruffman, A., and van Hinte, J. E. (1989). *Devonian Shelf-Depth Limestone Dredged from Orphan Knoll: A 1971 Discovery and a Reassessment of the HUDSON 78-020 Dredge Hauls from Orphan Knoll*. Ottawa: Geological Survey of Canada.

Sibuet, J.-C. (1992). New constraints on the formation of the non-volcanic continental Galicia-Flemish Cap conjugate margins. *Geol. Soc.* 149, 829–840. doi: 10.1144/gsjgs.149.5.0829

Smith, J. (1997). *The Use of Deep-Sea Corals in Paleooceanographic Monitors*. Ph.D. thesis, Department of Geology, McMaster University, Hamilton.

Smith, J. E. (1993). *Late Quaternary Climatic Reconstruction using the Deep-Water Coral Desmophyllum Cristigalli [sic]*. B.Sc. Honours thesis, Department of Geology, McMaster University, Hamilton.

Smith, J. E., Risk, M. J., Schwarcz, H., and McConnaughey, T. A. (1997). Rapid climate change in the North Atlantic during the younger dryas recorded by deep-sea corals. *Nature* 386, 818–820. doi: 10.1038/386818a0

Smith, J. E., Risk, M. J., Schwarcz, H., and McConnaughey, T. A. (2013). Corrigendum. *Nature* 502:258.

Srivastava, S., Verhoef, J., and Macnab, R. (1988). Results from a detailed aeromagnetic survey across the northeast Newfoundland margin. Part I: spreading anomalies and relationship between magnetic anomalies and the ocean-continent boundary. *Mar. Pet. Geol.* 5, 306–323. doi: 10.1016/0264-8172(88)90025-6

Taviani, M., Angeletti, L., Campiani, E., Ceregato, A., Foglini, F., Maselli, V., et al. (2012). Drowned karst landscape offshore the Apulian margin (southern Adriatic Sea, Italy). *J. Cave Karst Stud.* 74, 197–212. doi: 10.4311/2011jcks0204

Thompson, A. B., and Campanis, G. M. (2007). *Information on Fishing On and Around the Four Closed Seamount Areas in the NRA*. Dartmouth: North Atlantic Fisheries Organization.

Toews, M., and Piper, D. J. W. (2002). *Recurrence Interval of Seismically Triggered Mass-Transport Deposition at Orphan Knoll, Continental Margin off Newfoundland and Labrador*. Ottawa: Geological Survey of Canada Current Research.

van Hinte, J., Ruffman, A., van den Boogaard, M., Jansonius, J., van Kempen, T. M. G., Melchin, M. J., et al. (1995). Palaeozoic microfossils from Orphan Knoll, NW Atlantic Ocean. *Scr. Geol.* 109, 1–63.

van Rooij, D., Blamart, D., Kozachenko, M., and Henriet, J. (2007). "Small mounded contourite drifts associated with deep-water coral banks, Porcupine Seabight, NE Atlantic Ocean," in *Economic and Palaeoceanographic Significance of Contourite Deposits*, eds A. R. Viana, and M. Rebesco, (Geological Society: London), 225–244. doi: 10.1144/gsl.sp.2007.276.01.11

Wareham, V. E. (2009). *Identification guide to deep-sea corals: Newfoundland, Labrador and Baffin island, Canada*. Ottawa: Fisheries and Oceans Canada.

Welford, J. K., Shannon, M., O'Reilly, B. M., and Hall, J. (2012). Comparison of lithosphere structure across the Orphan Basin-Flemish Cap and Irish Atlantic conjugate continental margins from constrained 3D gravity inversions. *J. Geol. Soc.* 169, 405–420. doi: 10.1144/0016-76492011-114

Wielens, H., MacRae, A., and Shimield, J. (2002). Geochemistry and sequence stratigraphy of regional Upper Cretaceous limestone units, offshore eastern Canada. *Org. Geochem.* 33, 1559–1569. doi: 10.1016/s0146-6380(02)00103-1

Wiles, E., Green, A., Watkeys, M., Jokat, W., and Krocker, R. (2014). Anomalous seafloor mounds in the northern Natal Valley, southwest Indian Ocean: implications for the East African rift system. *Tectonophysics* 630, 300–312. doi: 10.1016/j.tecto.2014.05.030

Conflict of Interest: AR is owner and President of Geomarine Associates, Ltd., and declares no conflict of interest.

The remaining authors declare that the research was conducted in the absence of any commercial or financial relationships that could be construed as a potential conflict of interest.